Eur. Phys. J. Plus (2021) 136:410
https://doi.org/10.1140/epjp/s13360-021-01303-4

THE EUROPEAN PHYSICAL JOURNAL PLUS

Review

Accounting for the resistivity contribution of grain boundaries in metals: critical analysis of reported experimental and theoretical data for Ni and Cu

I. Bakonyi[a]

Institute for Solid State Physics and Optics, Wigner Research Centre for Physics, Konkoly-Thege út 29-33, Budapest 1121, Hungary

Received: 10 December 2020 / Accepted: 9 March 2021

Abstract In the present paper, reported literature data on the grain-size dependence of resistivity of Ni and Cu are critically evaluated by two conceptually different methods. One is the phenomenological approach of Andrews (Phys. Lett. 19: 558, 1965) according to which in a polycrystalline metal there is a resistivity contribution inversely proportional to the average grain diameter, the proportionality constant defined as the Andrews parameter A. The other method is the customary Mayadas–Shatzkes (MS) model (Phys Rev B 1: 1382, 1970) yielding a grain-boundary reflection coefficient R. During the analysis, special care was taken to rely only on data for which the surface scattering resistivity contribution was definitely negligibly small and the grain size was determined by direct microscopy imaging. By sorting out with this analysis the most reliable grain-size-dependent resistivity data for polycrystalline Ni and Cu metals with random grain boundaries, we have then derived the current best room-temperature values of the Andrews parameter A, the specific grain-boundary resistivity and the reflection coefficient R. We have also found a fairly good relation between the parameters A and R and compared the experimental values with their theoretical estimates reported in the literature. Then, the conceptual differences between the two approaches are discussed and the deficiencies of the MS model, especially in connection with the validity of Matthiessen's rule, are highlighted. A major conclusion is that by the Andrews method one can derive a model-independent reliable parameter characterizing the grain-boundary contribution to the resistivity of metals.

1 Introduction

The demand for the continuous downscaling of integrated circuits provides a permanent driving force for deepening our understanding of the resistivity of metals, especially Cu which is mainly used for fabricating interconnect lines. This well explains the recent interest in studying, both experimentally and theoretically, the contributions to the resistivity of Cu metal [1–4], although in search for alternative metals, general considerations have been extended to several other metals as well [5].

[a] e-mail: bakonyi.imre@wigner.hu (corresponding author)

Published online: 19 April 2021

An inevitable resistivity contribution from surface scattering effects in finite-size conductors such as thin films and wires, towards which currently used interconnect lines tend to approach, has long been recognized experimentally and has been incorporated into the model elaborated by Fuchs [6] and Sondheimer [7] and later further refined by including also surface roughness effects [8–11]. The Fuchs–Sondheimer (FS) model predicts a resistivity increase from surface scattering effects which is roughly proportional to the inverse of the film thickness or the wire diameter. Below a certain cross-sectional size of the interconnect lines, this geometrical size effect always contributes to the wire resistivity and its magnitude can only be controlled by the degree of specular reflection at the outer surfaces of the wire, mainly determined by the surface roughness. In recent decades, there has been a progress in treating the surface scattering in the frame of several quantum versions of the FS model which were summarized by Munoz and Arenas [2]. These authors have even further advanced the lastly developed quantum FS model by removing the constraint of any adjustable parameter and by using instead the currently available almost atomic-resolution surface roughness data from experiments.

In polycrystalline materials, there are, furthermore, also internal surfaces mainly in the form of grain boundaries. As any kind of lattice defects, also these two-dimensional lattice imperfections give a contribution to the resistivity since they represent additional scattering centers for the electrons carrying the current in metallic conductors [12].

A grain boundary constitutes a significant obstacle along the motion of the electrons. This is because the crystal lattice orientation with respect to the wave vector of the incoming electron is different on both sides of the grain boundary [12], so the electron should unavoidably undergo an appreciable scattering event when impinging on a grain boundary. Therefore, the smaller the grain size, the more grain boundaries are present in a crystalline material and, then, the larger the resistivity is. Interconnect lines are predominantly produced via atom-by-atom deposition processes such as sputtering, evaporation or electrodeposition. On the other hand, it has long been known that such deposits typically exhibit an average lateral grain size in the submicron range [13]. Thus, a significant resistivity contribution may also arise due to the large amount of grain boundaries as a consequence of the small grain size in these nanocrystalline (nc) metals. It is, therefore, inevitable to gather information on the magnitude of the grain-boundary contribution to the total resistivity.

The grain-boundary contribution to the resistivity has been usually evaluated by the classical Mayadas–Shatzkes (MS) model [14] yielding a grain-boundary reflection coefficient (R). The other approach to the grain-boundary resistivity derives from the observation of Andrews [15] who demonstrated that in a polycrystalline metal, there is a resistivity contribution (ρ_{GB}) proportional to the grain-boundary surface area per unit volume. Andrews defined the proportionality constant as the specific grain-boundary resistivity ρ_{SGBR} which, according to stereological considerations, is inversely proportional to the average grain diameter d. In a recent paper [16], when analyzing the resistivity data for nc-Ni metal samples with various grain sizes, we have introduced an Andrews parameter A via the relation $\rho_{SGBR} = A/d$. The frameworks of the grain-boundary resistivity analysis of reported experimental grain-size-dependent resistivity data by the two approaches (Andrews method and MS model) will be described in more detail in "Appendix A" where the connection between the Andrews parameter A and the grain-boundary reflection coefficient R will also be discussed.

Unfortunately, when reviewing relevant data, one can find a very large scatter of the reported parameters derived for characterizing the grain-boundary contribution to the resistivity in metals. Therefore, one purpose of the present paper is (1) to carry out a systematic analysis of the reported grain-size dependence of the resistivity data on two selected metals,

namely Ni and Cu and (2) to point out the sources of error which may have caused the fairly large scatter of the reported grain-boundary resistivity values.

Furthermore, particular attention will be paid to analyzing each data set by using both above mentioned approaches (the MS model [14] and the Andrews method [15]). A comparison of the grain-boundary resistivity parameters derived by these two approaches for a given metal (grain-boundary reflection coefficient R and Andrews parameter A, respectively) has not yet been made although this might greatly help us better identify the virtues and weaknesses of the two approaches. It will turn out from this comparison that whereas the Andrews method yields in a very straightforward manner a well-defined experimental parameter value for characterizing the grain-boundary contribution to the resistivity, the application of the very popular MS model [14] has not always been satisfactorily performed as pointed out already by Sambles [17] and this fact may have also contributed to the large scatter of available relevant R data for a given metal.

Therefore, for both metals, we will separately consider reported data for thin films and massive samples, the latter ones having macroscopic dimensions (at least in the micrometer range in every direction such as, e.g., typical for electrodeposited foils) so that the surface scattering effects can be safely neglected which is not always the case for thin films. As to the thin film data, they will be critically discussed and those data will only be included in the process of evaluating the grain-boundary resistivity parameters for which we can be convinced that the reported experimental results contain at most a negligibly small contribution from surface scattering effects to the measured resistivity. This is because we are interested in this paper in the resistivity contribution of a metal due to grain boundaries only. Furthermore, it should be noted that the resistivity results to be analyzed were mostly obtained on polycrystalline samples. Therefore, the derived parameters refer to the grain-boundary resistivity contribution averaged over all type and orientation of grain boundaries, i.e., these parameters characterize the scattering properties of so-called random grain boundaries. Where data are available for a specific type of grain boundary, we will mention it explicitly.

Another important issue is the microstructure evaluation method since, as pointed out in a recent paper [16] and further elucidated in "Appendix B", from the viewpoint of the electrical transport, the relevant parameter is the mean grain size d obtained from directly imaging the grains by, e.g., transmission electron microscopy (TEM) or electron back-scattering diffraction (EBSD) techniques. Therefore, in the main part of the paper, only those reported results will be discussed where the grain size determined by such imaging methods was reported, whereas an analysis of reports where X-ray diffraction (XRD) was only used for structural characterization will follow in "Appendix B".

It is also noted that there are several conceptual difficulties with the classical MS model [14] which were raised in the literature already long time ago [18–20] and also more recently by Munoz and Arenas [2] which authors have also elaborated a quantum theory of electron scattering in the presence of grain boundaries. Nevertheless, we will rely on the classical form of the MS theory since the vast majority of experimental results on grain-boundary resistivity parameters have been evaluated in this model and we will often use the reported MS parameters for reconstructing the evolution of resistivity with grain size if these data have not been explicitly included in the report considered. A critical discussion of the classical MS model including the conceptual difficulties of the model assumptions and the controversies arising from the model will be presented in a separate section.

It is believed that the present analysis of the grain-size dependence of the resistivity data for the two selected metals (Ni and Cu) will open up the way to collect more reliable data for all other metals along the same line which then can be used as a proper basis for testing theoretical models for calculating the grain-boundary contribution to the resistivity.

The paper is organized as follows. In Sect. 2, available experimental data sets will be analyzed for Ni and Cu metals by using both data analysis approaches (Andrews method and MS model). The procedure will be that we shall start with the discussion of those reports where direct resistivity (ρ) vs. grain size (d) size data were given. Then, we shall examine works in which some deduced parameters were only given and will attempt to reconstruct the original experimental $\rho_{exp}(d)$ data sets from which the parameter extraction had been carried out. Section 3 is devoted to comparing the parameters of the two approaches with each other for a given metal and separately both grain-boundary resistivity parameters (A and R) for each of the two metals Ni and Cu. In Sect. 4, the extracted experimental grain-boundary resistivity parameters of Ni and Cu will be confronted with the results of theoretical calculations of the specific grain-boundary resistivity for various types of grain boundaries for these two metals. Some general comments with criticism will be given on the two data evaluation approaches in Sect. 5 where some open issues will also be mentioned. A summary will then be given in Sect. 6.

In "Appendix A", the Andrews method and the MS model elaborated to deduce the contribution of grain boundaries to the resistivity will be introduced and the relation between their parameters will be discussed. In "Appendix B", a comparison of the microstructural parameters by TEM/EBSD and XRD will be made and those experimental reports will be evaluated where only the XRD crystallite size x was provided. In "Appendix C", an attempt will be made to estimate the maximum resistivity which can be achieved in nc-Ni and nc-Cu at the smallest grain sizes.

2 Evaluation of available grain-size-dependent resistivity data by the two approaches

2.1 Nickel

2.1.1 Ni resistivity data evaluated by the Andrews method

The currently available resistivity data for nc-Ni samples for which the grain sizes (d) were determined by TEM imaging are displayed in Fig. 1. The data reported in Ref. [16] and Refs. [21–25] were obtained on electrodeposited nc-Ni samples. For these data, an analysis according to the Andrews method was performed in Ref. [16] by fitting to Eq. (6) of "Appendix A" of the present paper. For the fitting, the standard value $\rho_{bulk}(\text{Ni};300\ \text{K}) = 7.24\ \mu\Omega\ \text{cm}$ [26] was used for bulk Ni resistivity and the fit yielded for the Andrews parameter $A(\text{Ni};300\ \text{K}) = 14.7 \times 10^{-16}\ \Omega\text{m}^2$ [16]. The fit is displayed in Fig. 1 by the thin solid line extending from 10 nm up to the highest grain size.

After publishing Ref. [16], we have found further literature data for the grain-size dependence of Ni obtained on thin films. Tochitskii and Belyavskii [27] investigated the room-temperature resistivity of 120-nm-thick evaporated Ni films by varying the grain size with substrate temperature during deposition or by gradually annealing the samples and the grain size d was determined by TEM. By plotting the resistivity as a function of the inverse grain size, i.e., according to the Andrews method (see "Appendix A.1", Eq. 6), they derived $A(\text{Ni};300\ \text{K}) = 14.8 \times 10^{-16}\ \Omega\text{m}^2$ and the corresponding fit function is indicated in Fig. 1 by the thick solid line over their grain size range (7 to 75 nm) which completely overlaps with the fit function obtained for the electrodeposited nc-Ni data (thin solid line over the whole grain size range).

We have evaluated also the data of de Vries [28] who investigated the resistivity of evaporated Ni thin films with various thicknesses from 10 to 80 nm both in the as-deposited and

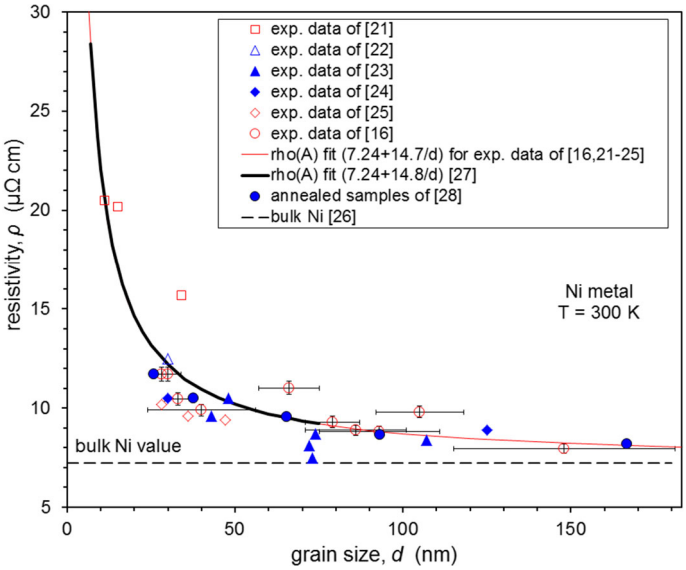

Fig. 1 Resistivity ρ at room temperature for Ni as a function of the grain size d. The thin solid line extending over the whole grain size range represents the fit according to the Andrews method to Eq. (6) with fixed $\rho_{\text{bulk}} = 7.24\ \mu\Omega$ cm and with fitted value $A = 14.7 \times 10^{-16}\ \Omega\text{m}^2$ for the data of Ref. [16] and Refs. [21–25]. The thick solid line represents the fit result of Ref. [27] on Ni thin films with $A = 14.8 \times 10^{-16}\ \Omega\text{m}^2$ in the investigated grain-size range (7 to 75 nm). The solid circles are the experimental data of Ref. [28] on annealed Ni thin films

annealed state (400 °C, 30 min in vacuum) as a function of temperature from 4 to 320 K. To prevent oxidation and gas adsorption at the film surface, a 20-nm-thick protecting SiO_2 layer was deposited in situ on top of the samples which is of great importance for the thinner films studied. The grain size d was evaluated by TEM and although no direct grain size data were reported, it was noted that for the annealed films the grain size was found to be 2.1 times the film thickness (for the as-deposited state, no quantitative data for the grain size were given). The reported room-temperature $\rho_{\text{exp}}(d)$ data for the annealed films of de Vries [28] are displayed in Fig. 1 by the solid circles which match very well all the other data [16, 21–25, 27].

Although the data for the electrodeposited nc-Ni samples show a rather large scatter, it is evident that a fit to these data (thin solid line) matches perfectly with the fit result from Ref. [27] and the data points of Ref. [28] are also well compatible with these fit results. Therefore, we can ascertain that the fit result $A(\text{Ni};300\ \text{K}) = 14.7 \times 10^{-16}\ \Omega\text{m}^2$ properly represents the best average value for the Andrews parameter characterizing the grain-boundary contribution to the resistivity in polycrystalline Ni metal with random grain boundaries at room temperature. Due to the good match of the nc-Ni thin film data [27, 28] with the average of the electrodeposited nc-Ni data [16, 21–25] also suggests that the actual error of the A(Ni;300 K) value is much less than indicated by the large scatter of the data in Fig. 1 and we may estimate this error to be about $\pm$ 10%. The reliability of the above average A(Ni;300 K) value is further justified by the fact that it was derived from the results of four independent laboratories (Erb and coworkers [21, 25], Bakonyi and coworkers [22–24], Tochitskii and Belyavskii [27] and de Vries [28]).

There are numerous further reports on the resistivity of Ni thin films (see, e.g., the review by Angadi [29]) which are not considered here individually. This is because the results are mostly not presented in the form of resistivity vs. grain size data, but rather just some extracted parameters (mostly grain-boundary reflection coefficient R) are given or the structural characterization was performed by XRD only and, therefore, their discussion will appear in "Appendix B". Apart from the effect of possible gaseous impurities during thin film deposition on the resistivity as discussed, e.g., in Ref. [30], for very thin films also the geometrical size effect comes into play and the evaluation was not always carefully carried out which may have often led to incorrect deduced data as pointed out by Sambles [17].

It is noted that according to Eq. (6), $\rho_{GB} = A/d$ predicts an extremely large resistivity for very small grain sizes what is physically unrealistic. Therefore, in "Appendix C" we shall make an estimate of the maximum possible room-temperature resistivity of Ni metal on the basis of the above derived A value.

As to the temperature dependence of the Andrews parameter A, we have analyzed the resistivity data for the annealed Ni films as reported by de Vries [28] for various temperatures. By using his reported resistivity data as a function of the grain size, we deduced the following values for the Andrews parameter: $A(\text{Ni};300\ \text{K}) = 12.2 \times 10^{-16}\ \Omega\text{m}^2$, $A(\text{Ni};77\ \text{K}) = 11.5 \times 10^{-16}\ \Omega\text{m}^2$ and $A(\text{Ni};4\ \text{K}) = 10.5 \times 10^{-16}\ \Omega\text{m}^2$. These data indicate an increase of A(Ni) by about 10% from 4 to 77 K and by about 16% from 4 to 300 K. Since de Vries [28] actually reported the temperature dependence of resistivity for various grain sizes, the dependence of A(Ni) on temperature could also be traced out in detail from these data.

2.1.2 Ni resistivity data evaluated by the Mayadas–Shatzkes model

As already mentioned above, numerous studies have been reported on the resistivity of Ni thin films and in most of these studies, a value of the grain-boundary reflection coefficient R was also deduced in the framework of MS model [14]. However, there is a very large scatter of the reported R(Ni) values ranging from 0.18 to 0.98 (see, e.g., the review by Angadi [29] and references therein). Since by definition $0 < R < 1$, such a broad range of the R values does not provide any useful parameter if we want to compare the grain-boundary contributions of different metals or the experimental data for a given metal to theoretically derived relevant values. Therefore, we should look for possible sources of error resulting in the large scatter of the R values reported for Ni metal and to deduce a reliable R(Ni) value if possible.

Our starting point for evaluating the grain-boundary reflection coefficient R of Ni metal in the framework of the classical MS model [14] is the known experimental grain-size dependence of the resistivity of polycrystalline Ni metal with random grain boundaries. This $\rho_{exp}(d)$ dependence was established in Sect. 2.1.1 and can be described by the average Andrews parameter $A(\text{Ni};300\ \text{K}) = 14.7 \times 10^{-16}\ \Omega\text{m}^2$ according to Eq. (6) where the total resistivity ρ_A in the Andrews approach is given as $\rho_A = \rho_{bulk} + A/d$ with the standard bulk resistivity $\rho_{bulk}(\text{Ni};300\ \text{K}) = 7.24\ \mu\Omega\ \text{cm}$ [26]. This grain-size-dependent average resistivity of Ni metal, $\rho_{exp}(d)$, is given in Fig. 1 by the thin solid line.

The background and assumptions of the MS model [14] are summarized in detail in "Appendix A.2". Here we recall only that in the MS model [14] the resistivity $\rho_{MS}(d)$ depends on the grain size d through a parameter α only where $\alpha = (\lambda_{bulk}/d)\ R/(1-R)$ as defined by Eq. (10). In the last expression, ρ_{bulk} is the electron mean free path (emfp) in the bulk state at the temperature of the experiment and R is the electron reflection coefficient from a grain-boundary wall and R depends on the scattering potential of the grain boundary. The simplest way of deriving the reflection coefficient R from the experimental $\rho_{exp}(d)$ data is to calculate the $\rho_{MS}(d)$ resistivity as a function of the grain size d for various R

values with constant λ_{bulk} corresponding to the mean free path of the metal under study at the measurement temperature. These calculated $\rho_{MS}(d)$ functions are then compared to the measured $\rho_{exp}(d)$ curves to find the R value for which $\rho_{MS}(d)$ matches best the $\rho_{exp}(d)$ data.

The most serious complication entering the reflection coefficient evaluation by the MS model [14] is that, according to Eq. (10), the value of the electron mean free path (λ_{bulk}) also determines the calculated value of the resistivity $\rho_{MS}(d)$ for a given R value. When reviewing the literature studies where R data were reported for Ni, it turns out that widely different values were used for λ_{bulk}(Ni;300 K). The real value of this parameter is a critical issue even today. Eq. (2.91) of the book of Ashcroft and Mermin [31] provides a formula for the free-electron estimate of the electron mean free path from which, with the electron density parameter they gave for Fe and with ρ_{bulk}(Ni,300 K) = 7.24 μΩ cm [26], we get λ_{bulk}(Ni;300 K) = 5.71 nm. This free-electron estimate is fairly close to the λ_{bulk}(Ni;300 K) = 5.62 nm value derived from the calculated product $[\rho_{bulk}\ \lambda_{bulk}]_{Ni} = 4.07 \times 10^{-16}$ Ωm^2 of Gall [5]. The temperature-independent product $[\rho_{bulk}\lambda_{bulk}]_{Ni}$ was derived [5] from the bulk electronic structure of Ni obtained from first-principles density-functional calculations which correctly account for the anisotropy in the Fermi surface as well as the variation in the electron velocity as a function of the electron wave vector.

Experimentally, the electron mean free path is determined, e.g., by measurements of the resistivity of thin films in the thickness range where surface scattering is expected to be significant and then applying the FS model [6, 7]. As already noticed by Sambles [17], this is not a straightforward procedure since the unknown value of the surface scattering specularity parameter enters the FS fit [6, 7] as well as simultaneously the influence of grain-boundary scattering being usually significant for thin films and treated by the MS model [14] should also be taken into account.

In order to simplify the problem, Milosevic et al. [32] made efforts to produce epitaxial Ni thin films which were practically single crystals since in this case one gets rid of at least the grain-boundary resistivity contribution. From this analysis, these authors [32] have derived the mean free path values λ_{bulk}(Ni;295 K) = 26 ± 2 nm and λ_{bulk}(Ni;77 K) = 350 ± 20 nm. In a more recent paper, Gall [33] has made serious considerations about the electron mean free path and has come to the conclusion that the large discrepancy (a factor of about 4.5) between the calculated and experimental value of λ_{bulk}(Ni) at a given temperature may be due to a breakdown of the classical FS [6, 7] transport model for small dimensions or imperfections of the experimental samples including crystalline defects, surface roughness, or variations in the surface scattering specularity. Concerning the shortcomings of the classical transport models [6, 7, 14], Gall [33] noted that these lead to an overestimation of the λ_{bulk} value when applying the FS model to fitting the experimental ρ vs. layer thickness data for small layer thicknesses. Therefore, the effective mean free path (λ_{eff}) determined from such experiments is not necessarily an actual mean free path of the bulk metal, but just a fitting parameter which describes properly the observed thickness dependence of the resistivity. These difficulties were discussed also by Munoz and Arenas [2] when refining the quantum mechanical extension of the FS model [6, 7] and relying on the experimental surface roughness data.

After these introductory considerations, we will now evaluate the reflection coefficient R of grain boundaries in Ni metal by carrying out an MS fit to the experimental $\rho_{exp}(d)$ data. As noted above, the average experimental resistivity of Ni metal, ρ_{exp}, depends on the grain size d as represented by Eq. (6) $\rho_{exp} = \rho_{bulk} + A/d$ with parameters ρ_{bulk}(Ni;300 K) = 7.24 μΩ cm [26] and A(Ni;300 K) = 14.7×10^{-16} Ωm^2. These $\rho_{exp}(d)$ data represented by Eq. (6) with the above two parameter values are displayed in Fig. 2 by the solid line.

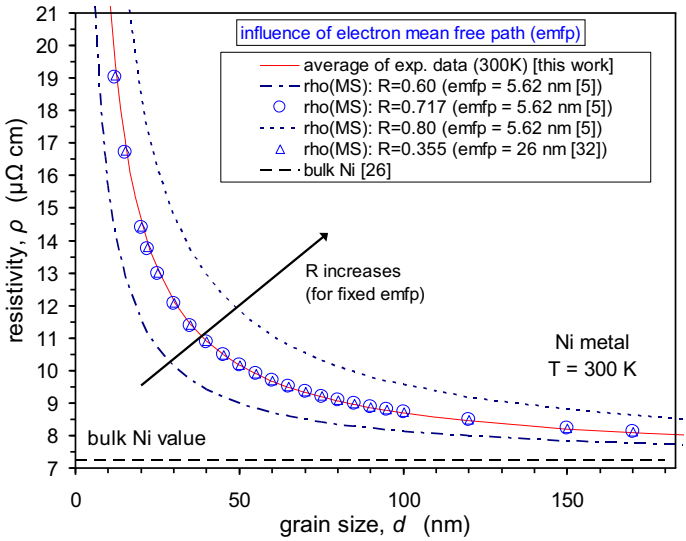

Fig. 2 Resistivity ρ at room temperature for Ni as a function of the grain size d. The solid line represents the average experimental data $\rho_{\mathrm{exp}}(d)$ from a fit according to the Andrews method [15] to Eq. (6) with fixed $\rho_{\mathrm{bulk}} = 7.24\ \mu\Omega$ cm [26] and with fitted value $A = 14.7 \times 10^{-16}\ \Omega\mathrm{m}^2$ for the data presented in Fig. 1. The open circles represent the $\rho_{\mathrm{MS}}(d)$ data according to Eq. (8) of the MS model [14] for a calculated electron mean free path (emfp) value of 5.62 nm [5] with $R = 0.717$, which match very well the average experimental data. The dash-dot line and the thin dashed line represent $\rho_{\mathrm{MS}}(d)$ curves for $R = 0.6$ and 0.8, respectively, for the same emfp value. The arrow indicates the direction of the increase of R for a fixed emfp value. The open triangles demonstrate that the average experimental data can be very well fitted to the MS model [14] also for the experimental emfp value of 26 nm [32] if the reflection coefficient is chosen as $R = 0.355$

For a fit of the average resistivity vs. grain size data (ρ_{exp}) to the MS model [14], we have calculated several $\rho_{\mathrm{MS}}(d)$ curves corresponding to Eq. (8) with different R values first by using the theoretical value $\lambda_{\mathrm{bulk}}(\mathrm{Ni};300\ \mathrm{K}) = 5.62$ nm by Gall [5]. One can see in Fig. 2 that the $\rho_{\mathrm{MS}}(d)$ data with $R = 0.717$ (open circles) perfectly superimpose on the solid line representing the average of the experimental data $\rho_{\mathrm{exp}}(d)$ for Ni. Therefore, the grain-boundary reflection coefficient for Ni is found to be $R = 0.717$ at room temperature by using the calculated mean free path of Gall [5]. We have carried out the same MS fit by using the experimental mean free path of Ni $\lambda_{\mathrm{bulk}}(\mathrm{Ni};295\ \mathrm{K}) = 26$ nm as given by Milosevic et al. [32] and the resulting $\rho_{\mathrm{MS}}(d)$ data with $R = 0.355$ (open triangles) also nicely agree with both the average experimental resistivity data ρ_{exp} (solid line) and the $\rho_{\mathrm{MS}}(d)$ data obtained with the theoretical electron mean free path value (open circles).

With reference to Fig. 2, we can conclude that both the MS model [14] and the Andrews method [15] describe equally well quantitatively the grain-size dependence of the resistivity for Ni metal for various chosen values of the mean free path in the MS model. Nevertheless, we should keep in mind that the fit parameters of the two data evaluation approaches have different physical meanings and we will look for a relation between the Andrews parameter A and the reflection coefficient R which will be done in "Appendix A.3".

We can also infer from Fig. 2 that different assumed values of the electron mean free path obviously lead to different R values (for the current choices of the mean free path, the R values differ by a factor of about 2). We have also carried out a series of MS fits to the average room-temperature experimental data $\rho_{\mathrm{exp}}(d)$ of Ni by using λ values ranging from

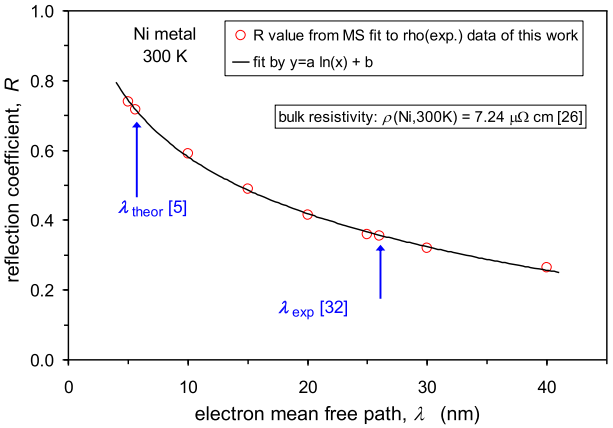

Fig. 3 Dependence of the grain-boundary reflection coefficient R of Ni metal (open circles) on the assumed value of the electron mean free path λ from fitting the average room-temperature resistivity data ρ_{exp}(d) for Ni with the MS model [14]. The solid line over the R vs. λ data is just an empirical fit corresponding to the relation $R = -0.2344 \cdot \ln(\lambda) + 1.1212$ where λ is taken in nanometer units

5 nm (close to the theoretically calculated value of Gall [5]) to 40 nm (somewhat beyond the experimental value of Milosevic et al. [32]) and determined for each λ value the reflection coefficient R for which the $\rho_{MS}(d)$ curve matches the average experimental $\rho_{exp}(d)$ data.

The dependence of the reflection coefficient R on the electron mean free path λ obtained in this manner for Ni metal at room temperature is displayed in Fig. 3. There is a smooth variation of R in a wide range as a function of λ and this variation can be described, just to quantify it without any physical model, by the relation $R = -0.2344 \cdot \ln(\lambda) + 1.1212$ where λ is taken in nanometer units.

As was already noted, in previous studies of the grain-boundary scattering effect on the resistivity of Ni, various electron mean free path values typically between the above two extremes (λ_{bulk}(Ni;300 K) = 5.62 nm [5] and λ_{bulk}(Ni;295 K) = 26 nm [32]) were used. Therefore, in view of the strong dependence of R on λ_{bulk}, these reported R values should be considered with significant caution. Even from our average $\rho_{exp}(d)$ data for Ni, we cannot extract a correct value for R(Ni) until we cannot be sure about the real value of the electron mean free path of bulk Ni.

As for the further literature data on the reflection coefficient of Ni metal, we will test first the R(Ni,300 K) = 0.40 value reported by Tochitskii and Belyavskii [27] whose $\rho_{exp}(d)$ data for Ni films with a thickness of 120 nm completely agree with the reference experimental data as is demonstrated in Fig. 1. These authors used λ_{bulk}(Ni;300 K) = 21.5 nm for carrying out the MS fit to their resistivity data according to Eqs. (8)–(10). They have neglected any surface scattering effects which is justified due to their high film thickness. When calculating the R(Ni) value corresponding to this mean free path from the relation describing the dependence of R on λ according to Fig. 3, we end up with exactly R(Ni,300 K) = 0.40. This shows the consistency of the derived Andrews parameter and reflection coefficient data of Ref. [27] although their derived R(Ni) value reflects only the arbitrary choice of the electron mean free path. Since the experimental resistivity vs. grain size data of Tochitskii and Belyavskii [27] match perfectly our reference data (see Fig. 1), the R(Ni) value of their samples is the same as the reflection coefficient of random grain boundaries the actual value of which, however, remains to depend on the choice of the electron mean free path of Ni.

We note that since also the $\rho_{exp}(d)$ data of de Vries [28] for the annealed Ni films fairly well overlap with the reference data (see Fig. 1), the R(Ni) value of these films is expected to have the same R(Ni) value. The reported result [28] was $R(\text{Ni}) = 0.44$ for the annealed films due to the particular choice of the electron mean free path. The procedure of de Vries [28] was that the temperature dependence of the resistivity from 4.2 K to 300 K was fitted by using the MS model as given by Eqs. (8)–(10). It was mentioned that surface scattering effects were found to be negligible. The electron mean free path $\lambda_{bulk}(T)$ at each measuring temperature was calculated from the product $[\rho_{bulk}\lambda_{bulk}]_{Ni} = 8.17 \times 10^{-16}$ Ωm^2 assumed to be temperature independent as is usually the case. By taking the standard $\rho_{bulk}(\text{Ni};300\text{ K}) = 7.24\ \mu\Omega$ cm [26] value, the chosen product value corresponds to $\lambda_{bulk}(\text{Ni};300\text{ K}) = 11.3$ nm. With this electron mean free path, Fig. 3 suggests a reflection coefficient value of $R(\text{Ni}) = 0.55$ at room temperature, somewhat higher than deduced by de Vries [28] by relying on his measured resistivity data over a large temperature range. Anyway, the uncertainty of R(Ni) due to the unknown value of λ_{bulk}(Ni) remains further open.

We discuss briefly also the data of Islamgaliev et al. [34] who reported on a study of massive Ni specimens which were first subjected to a severe plastic deformation procedure to reduce the grain size and then gradually annealing to obtain various grain sizes. They evaluated the grain size by TEM and measured the resistivity at 77 K at each annealing stage. No direct grain size vs. resistivity data were given, they just reported a deduced value of $R = 0.38$ by using $\lambda_{bulk}(\text{Ni};77\text{ K}) = 110$ nm and $\rho_{bulk}(\text{Ni};77\text{ K}) = 0.72\ \mu\Omega$ cm, the former derived from the product $[\rho_{bulk}\lambda_{bulk}]_{Ni} = 8.17 \times 10^{-16}$ Ωm^2 and $\rho_{bulk}(\text{Ni};77\text{ K})$ measured on a Ni sample annealed at 1400 °C. By using the reported parameter values, we could reconstruct their average resistivity data as a function of grain size and they were in relatively good agreement with the resistivity data reported earlier for Ni at T = 77 K [21, 28] although in lack of more details of the measured ρ (d) data of Ref. [34], we cannot extract more information. Furthermore, similarly to the above discussed problem of the mean free path value of bulk Ni at 300 K, we face the same situation at 77 K since the theoretically calculated value is 81.5 nm [5], the experimental value is 350 nm [32] and an intermediate value (110 nm) was used by Islamgaliev et al. [34].

We could see above that the grain-boundary reflection coefficient of Ni can only determined via the classical MS model [14] if we shall have an exact value for the electron mean free path of bulk Ni. By considering the available theoretical and experimental estimates of $\lambda_{bulk}(\text{Ni};300\text{ K})$, we could only establish a possible range for the R(Ni) value: $0.355 \le R(\text{Ni}) \le 0.717$ even if we rely on the best average $\rho_{exp}(d)$ data for Ni as determined in the present paper. With reference to Fig. 2, it is clear that the even wider range of reported R(Ni) values as mentioned at the beginning of this section may have occurred due to several reasons. One evident reason comes from the various chosen values of the electron mean free path. It is also clear that even for a fixed value of λ_{bulk}(Ni), if the measured resistivity for a given grain size is larger than the reference $\rho_{exp}(d)$ data represented by the solid line in Fig. 2, the R(Ni) value from the MS fit will also be larger (and if the resistivity is smaller than the reference $\rho_{exp}(d)$ data, then the deduced R(Ni) value will also be smaller). It is well known that any kind of impurities and an increased surface roughness contribute to an increase of the resistivity. This is especially critical for thin films since the grain-boundary reflection coefficients were mostly determined on such specimens. As pointed out by Sambles [17], the evaluation of resistivity data for deriving the value of R(Ni) in the combined FS [6, 7] and MS [14] models has not been always carried out with proper care. Furthermore, in addition to emphasizing several aspects of the inadequacy of the classical FS and MS models, Munoz and Arenas [2] also demonstrated that the application of these classical models can lead to

ambiguous results in that several pairs of λ and R values give a MS fit of the experimental data with the same accuracy.

It is noted finally that, as mentioned in the Introduction, any further reports on the resistivity of Ni metal in which the grain size was not determined, only the crystallite size from XRD experiment, will be discussed in "Appendix B".

2.2 Copper

2.2.1 Cu resistivity data evaluated by the Andrews method

Andrews [15] investigated the grain-boundary contribution to the resistivity of on massive Cu samples and derived a value for the specific grain-boundary contribution ρ_{SGBR}(Cu) with the help of the formulae explained in "Appendix A.1". The grain sizes being in the micrometer range were determined by optical microscopy by not taking into account twin boundaries, and the resistivity was measured at 4.2 K. Later, Andrews et al. [35] reported a refined value $\rho_{SGBR}(\text{Cu;4.2 K}) = 3.12 \times 10^{-16}\ \Omega\text{m}^2$ which can be converted, by using their proportionality factor $k_{GB} = 2.7$ in Eq. (3), to $A(\text{Cu,4.2 K}) = 8.42 \times 10^{-16}\ \Omega\text{m}^2$.

Subsequently, there have been numerous studies for Cu mainly on thin film samples (see, e.g., the review by Angadi [29]), most of which suffer from the same deficiencies as discussed above for Ni thin films. Here, first we will rely on a recent study [1] in which the experimental data were carefully analyzed and the results turn out to be in fairly good conformity with the early findings of Andrews et al. [35]. Other results on Cu thin films and massive samples will be considered thereafter only.

Sun et al. [1] reported a detailed study of the electrical resistivity of sputtered Cu thin films with layer thicknesses in the range from about 27 to 158 nm and they have determined the grain sizes by TEM by averaging over typically 500 to 1500 grains. The lateral grain size was found to vary from about 35 to 425 nm, to some extent independently of the film thickness. These authors performed the data analysis by various combinations and extensions of the classical FS and MS models.

In this section, we shall analyze the data presented by Sun et al. [1] for Cu thin films by the Andrews method [15] as described in "Appendix A.1" for evaluating the grain-boundary contribution to the resistivity, similarly to the case of Ni in Sect. 2.1.1. The experimental data of Sun et al. [1] are displayed in Fig. 4 for both 296 and 4.2 K. The inset shows the resistivity results of another report (open triangles) for T = 273 K on sputtered nc-Cu films [36] with grain sizes from TEM imaging. There is a relatively good match of the two independent data sets (the difference being mainly due to the lower measurement temperature in Ref. [36]).

The solid lines in Fig. 4 obtained by fitting to Eq. (6) with fixed bulk Cu resistivity values as specified in the figure caption describe very well the experimental data of Sun et al. [1] at both temperatures. The normalized fit quality (NFQ) parameter provided by the Excel fitting program as the square of the Pearson product moment correlation coefficient was fairly close to unity in both cases (see caption to Fig. 4); the fit quality improved by less than 1% only when the bulk resistivity was not fixed. By taking $\rho_{bulk}(\text{Cu;RT}) = 1.72\ \mu\Omega$ cm [26] and $\rho_{bulk}(\text{Cu;4.2 K}) = 0\ \mu\Omega$ cm, we obtain the fit values as $A(\text{Cu,296 K}) = 8.69 \times 10^{-16}\ \Omega\text{m}^2$ and $A(\text{Cu,4.2 K}) = 7.22 \times 10^{-16}\ \Omega\text{m}^2$ for the experimental $\rho_{exp}(d)$ data of Sun et al. [1]. For the data of Fenn et al. [36], the same analysis with $\rho_{bulk}(\text{Cu;273 K}) = 1.546\ \mu\Omega$ cm [26] yields $A(\text{Cu,273 K}) = 8.77 \times 10^{-16}\ \Omega\text{m}^2$ (in the analysis, we have omitted the data for the two smallest grain sizes since these refer to very thin films which were mentioned in Ref. [36] to be eventually not continuous). The A(Cu,273 K) value for the Cu films of Ref. [36] is in good agreement with the A(Cu,296 K) value on the Cu films of Ref. [1].

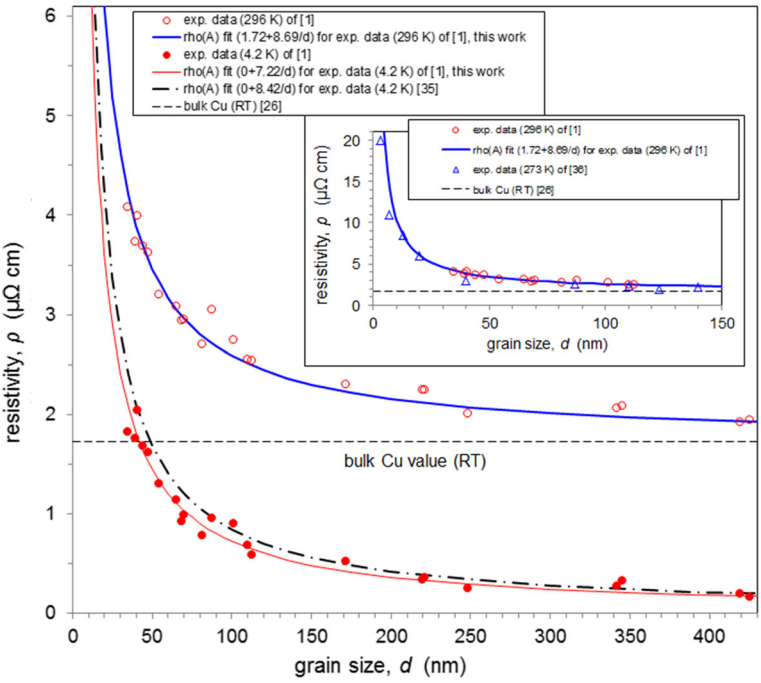

Fig. 4 Resistivity ρ for sputtered Cu films as a function of the grain size d [1]. Key to symbols: open circles (296 K); solid circles (4.2 K). The thick solid line represents a fit to Eq. (6) with fixed $\rho_{\text{bulk}}(300\ \text{K}) = 1.72$ $\mu\Omega$ cm value [26] and with fitted value $A = 8.69 \times 10^{-16}$ Ωm^2 for the data at 296 K (normalized fit quality parameter: NFQ = 0.968); the thin solid line represents a fit to Eq. (6) with fixed $\rho_{\text{bulk}}(4.2\ \text{K}) = 0$ $\mu\Omega$ cm and with fitted value $A = 7.22 \times 10^{-16}$ Ωm^2 for the data at 4.2 K (NFQ = 0.963). The dash-dot line represents the resistivity data of Andrews et al. [35] obtained at 4.2 K on massive Cu samples with grain sizes from 30 to 100 μm when extrapolated to the nanometer grain-size range by using their $A = 8.42 \times 10^{-16}$ Ωm^2 value. The inset shows the data (open triangles) of another report on Cu films [36], being in good agreement with the results of Sun et al. [1] by considering the difference in the measurement temperatures

Figure 4 reveals that the low-temperature data of Sun et al. [1] on thin films match fairly well the dash-dot line representing the data of Andrews et al. [35] on massive Cu specimens with $A(\text{Cu,4.2 K}) = 8.42 \times 10^{-16}$ Ωm^2 if the latter data are extrapolated to the nanometer grain-size range. This underlines, on the other hand, the conclusions of Sun et al. [1] in that for their Cu films the grain-boundary scattering was the really dominant effect in influencing the variation of resistivity with grain size and the surface scattering effects were practically negligible even for the thinnest films. We can also conclude from the close quantitative agreement of the low-temperature data of Sun et al. [1] and Andrews et al. [35] for a given grain size and of the two corresponding A(Cu;4.2 K) values that the Cu thin films studied by Sun et al. [1] were of high quality and free of the usual deficiencies, such as impurities and large surface roughness, usually resulting in high resistivities of thin films.

We can also see that for the nc-Cu films investigated by Sun et al. [1], the A(Cu) value increases by about 20% from 4.2 K to 296 K. It is noted that Andrews et al. [35] reported an increase of A(Cu) by 20% when raising the temperature from 4.2 K to 85 K. We recall from Sect. 2.1.1 that slightly smaller, but comparable increase of A(Ni) could be deduced from the data of de Vries [28]. All these data indicate that there is a slight, but apparently measurable temperature dependence of A for both Ni and Cu.

Based on the good matching of the thin film data of Sun et al. [1] with the results of Andrews et al. [35] on massive specimens at 4.2 K, we can consider the $\rho_{exp}(d)$ data of Sun et al. [1] for 296 K as well representing the real variation of the room-temperature resistivity with grain size for Cu metal with random grain boundaries. This is further supported with the good quantitative agreement of the Andrews parameter deduced from the data of Sun et al. [1] at $T = 296$ K with that from the data of Fenn et al. [36] at $T = 273$ K. Therefore, other reported results for the grain-size dependence of the resistivity of Cu will be discussed with reference to the $\rho_{exp}(d)$ data of Sun et al. [1] represented by the Andrews parameter $A(\text{Cu,296 K}) = 8.69 \times 10^{-16}\ \Omega\text{m}^2$.

We start with the resistivity results of Artunc and Öztürk [37] who established the grain size of evaporated Cu films (thickness range: 17 to 301 nm) by TEM. The grain-size dependence of the resistivity was found to agree fairly well for the as-deposited and annealed films as Fig. 5 reveals (open triangles). Although the evolution of resistivity with grain size seems to be very similar to that found by Sun et al. [1] whose results are considered as reference $\rho_{exp}(d)$ data for Cu and are represented by the thick solid line in Fig. 5, all the data of Ref. [37] fall below the reference data.. The lower resistivity values of Ref. [37] for any given grain size value can be related to the fact that these data could be fitted with the Andrews method with good fit quality only by using a room-temperature resistivity of 1.51 $\mu\Omega$ cm for bulk Cu which is definitely smaller than the standard value ($\rho_{bulk}(\text{Cu;RT}) = 1.72\ \mu\Omega$ cm [26]). It should be noted that the resistivity data of Artunc and Öztürk [37] at 100 K also yielded a lower value for infinitely large grain sizes than the standard bulk value at that temperature. A fit of Eq. (6) to the data of Artunc and Öztürk [37] yields a lower value for the Andrews parameter [$A(\text{Cu,300 K}) = 6.1 \times 10^{-16}\ \Omega\text{m}^2$] than the room-temperature value $A(\text{Cu}) = 8.69 \times 10^{-16}\ \Omega\text{m}^2$ derived from the reference $\rho_{exp}(d)$ data for Cu. The lower A(Cu) value from the data of Ref. [37] certainly comes partly from the fact that the Andrews fit yields a too low bulk resistivity value which may be eventually from an underestimated resistivity of these specimens.

Bruschi et al. [38] investigated evaporated Cu films with thicknesses 320 and 330 nm both in the as-deposited and annealed states and determined the grain size by TEM. Their data (open circles in Fig. 5) are somewhat above the reference $\rho_{exp}(d)$ data, mainly because of the larger fitted bulk resistivity (1.99 $\mu\Omega$ cm) than the standard bulk value (the authors ascribe the excess resistivity to the contribution of intragranular defects and impurities). On the other hand, due to the apparently weaker dependence of the resistivity on grain size in these samples, one can derive a much smaller value $A(\text{Cu,300 K}) = 5.0 \times 10^{-16}\ \Omega\text{m}^2$ than the reference value of $A(\text{Cu,296 K}) = 8.69 \times 10^{-16}\ \Omega\text{m}^2$.

Riedel et al. [39] investigated evaporated Cu films with thicknesses ranging from 250 to 900 nm. The films were produced by chemical vapor deposition (CVD) from a metal-organic precursor on Si wafers with various underlayers at a substrate temperature of 200 0C. The grain size established from TEM dark-field images ranged from 37 to 186 nm for their films. They observed a linear dependence of $\rho_{exp}(d)$ on $1/d$ from which the parameters $\rho_{bulk}(\text{Cu;300 K}) = 1.8\ \mu\Omega$ cm and $A(\text{Cu,300 K}) = 5.8 \times 10^{-16}\ \Omega\text{m}^2$ can be derived. The evolution of the $\rho_{exp}(d)$ data of Ref. [39] with grain size is displayed by the thin dashed line in Fig. 5 and they are fairly close to, but somewhat below the reference $\rho_{exp}(d)$ data.

Tochitskii and Belyavskii [27] reported an $A(\text{Cu,300 K}) = 3.90 \times 10^{-16}\ \Omega\text{m}^2$ value for evaporated Cu films with 90 nm thickness which were produced on substrates with various temperatures or annealed after deposition in order to have a range of grain sizes. Their data are represented by the thin solid line in Fig. 5 and they fall well below the reference $\rho_{exp}(d)$ data.

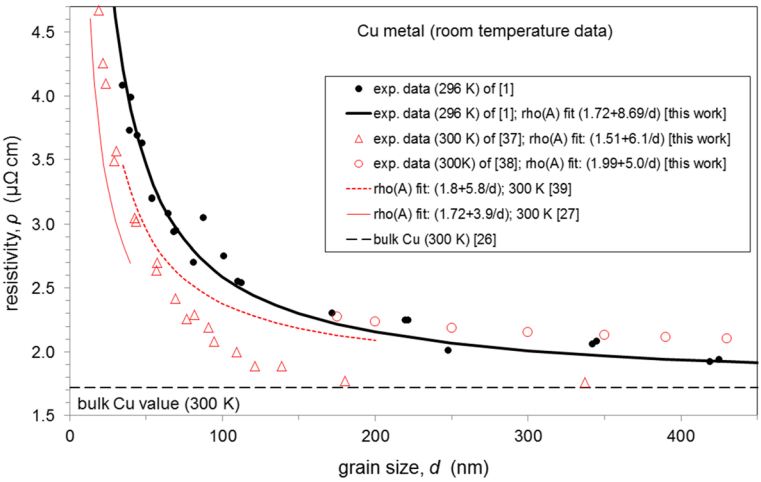

Fig. 5 Room-temperature resistivity ρ for various physically deposited Cu films as a function of the grain size d. Full circles are data at 296 K from Ref. [1] and the solid line represents a fit to Eq. (6) with fixed $\rho_{\text{bulk}} = 1.72\ \mu\Omega$ cm [26] and with fitted value $A = 8.69 \times 10^{-16}\ \Omega\text{m}^2$ for these data. For the experimental data from other studies, the end of the legend text provides the parameters of the Andrews fit according to Eq. (6) in the same units as above. The thin dashed and solid lines represent the experimental data of Refs. [39] and [27], respectively, over the investigated grain size range according to Eq. (6) with the reported parameter values

By looking at the data presented in Fig. 5, we can establish that the resistivity data of other reported studies show a fairly similar evolution with grain size as the reference $\rho_{\text{exp}}(d)$ data of Sun et al. [1] although most of the former ones have a lower value for a given grain size. We will come back to this point later, after discussing first the $\rho_{\text{exp}}(d)$ data reported for electrodeposited Cu layers [40–42] which are displayed in Fig. 6 where also the reference $\rho_{\text{exp}}(d)$ data obtained on evaporated Cu films [1] are included by the thick solid line.

Wu et al. [40] investigated narrow Cu strips with thicknesses in the range 100 to 300 nm and widths ranging from 100 to 300 nm which were electrodeposited into patterned trenches. The Cu strips were subsequently annealed at 250 °C for 30 s and the grain size was established by focused ion-beam (FIB) imaging. The reported resistivity vs. grain size data displayed by the large open diamond symbols in Fig. 6 are above the reference $\rho_{\text{exp}}(d)$ line. From the Andrews fit (thin line with small full diamond symbols), we obtain a resistivity $\rho_{\text{bulk}}(\text{Cu}) = 1.91\ \mu\Omega$ cm for large grain sizes which is larger than the standard bulk value ($1.72\ \mu\Omega$ cm [26], whereas the Andrews parameter [$A(\text{Cu},300\ \text{K}) = 9.7 \times 10^{-16}\ \Omega\text{m}^2$] is slightly higher than the reference value [$A(\text{Cu},300\ \text{K}) = 8.69 \times 10^{-16}\ \Omega\text{m}^2$]. It was noticed by Wu et al. [40] that there was a resistivity contribution from sidewall surface scattering since the resistivity strongly increased with decreasing strip width. This may partly explain their higher resistivities with respect to the reference values although the authors have commented also on the possible role of impurities which may have accumulated preferably in the grain boundaries upon annealing and leading to higher grain-boundary resistivity contribution and also to a higher A(Cu) value.

Woo [41] investigated the room-temperature resistivity of large-area electrodeposited Cu layers with 25 μm thickness by using pulse-plating (PP) deposition. The grain size was determined by TEM from dark-field images and the results are displayed in Fig. 6 by large open squares. By performing the Andrews fit (thin line with small full square symbols), it is surprising that whereas the resistivity for large grains ($\rho_{\text{bulk}}(\text{Cu}) = 1.81\ \mu\Omega$ cm) remains

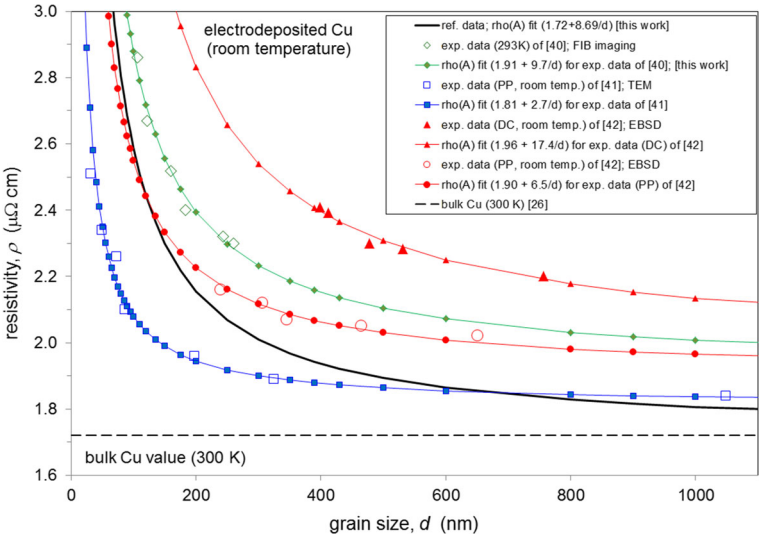

Fig. 6 Room-temperature resistivity ρ for various electrodeposited Cu films as a function of the grain size d evaluated by TEM, EBSD or FIB imaging as indicated in the legend. The notations DC and PP refer to direct-current and pulse-plating electrodeposition. The thick solid line represents the reference $\rho_{\mathrm{exp}}(d)$ data at 296 K. The various data and their Andrews fits (thin lines with symbols) are discussed in the text

above the standard bulk Cu value, the Andrews parameter is extremely small [$A(\mathrm{Cu}) = 2.7 \times 10^{-16}$ $\Omega\mathrm{m}^2$], it is less than one third of the reference value [$A(\mathrm{Cu},300\ \mathrm{K}) = 8.69 \times 10^{-16}$ $\Omega\mathrm{m}^2$]. This indicates that the grain-boundary resistivity in these deposits is much smaller than that of the average random grain boundaries in Cu.

After investigating in more detail the grain-boundary character distribution in these samples, Woo [41] came to the conclusion that the relatively small resistivity values at lower grains sizes may be a result of a large fraction of such specific grain boundaries which are usually termed as coincident site lattice (CSL) boundaries in which the two adjacent crystallites share many common atomic positions, i.e., they are much more "ordered" than an average random grain boundary. A larger degree of topological order in the grain boundary naturally implies a lower resistivity contribution by the grain boundary. It has been, indeed, pointed out by Nakamichi [43] via measurement of the grain-boundary resistivity of individual grain boundaries in Al metal bicrystals that more ordered grain boundaries exhibit a lower resistance than less ordered ones. Woo [41] found that by reducing the grain size, the fraction of these special, more ordered grain boundaries increased in the investigated samples. The presence of a large fraction of such more ordered boundaries then may explain the much lower $A(\mathrm{Cu})$ value obtained from these data.

Dela Pena and Roy [42] investigated the room-temperature resistivity for large area electrodeposited Cu layers with 25 μm thickness and they determined the grain size by electron backscatter diffraction (EBSD) imaging. Their results are displayed in Fig. 6 by large full triangles and large open circles corresponding to samples produced by direct-current (DC) plating and pulse plating (PP), respectively. It can be seen that at the same average grain size, the PP samples exhibit lower resistivities. Both data sets could be well fitted with the Andrews method according to the Eq. (6) as indicated by the thin lines with small full triangles and circles, respectively, over the corresponding data points. The large-grain resistivity from the fit was to be around 1.9 μΩ cm for both the DC and PP samples, i.e., by about 0.2 μΩ cm

larger than the bulk value for pure Cu, whereas the Andrews parameter was quite different for the two kinds of samples: $A(\mathrm{Cu,DC}) = 17.4 \times 10^{-16}$ $\Omega\mathrm{m}^2$ and $A(\mathrm{Cu,PP}) = 6.5 \times 10^{-16}$ $\Omega\mathrm{m}^2$. Apparently, in this case the deposition method (DC or PP) has significantly influenced the average resistivity contribution by grain boundaries which may be due two reasons. If the excess resistivity over the bulk value arises from eventual impurities in the deposit, then it may be that the DC and PP deposition modes differently act on the nucleation process and this leads then to a difference in the amount of impurities incorporated in the grain boundaries. The other possibility is that the eventual presence of impurities in the grain boundaries is roughly the same, but the DC and PP deposition modes lead to different fractions of the more ordered and less ordered grain boundaries (see the above discussed work of Woo [41]). If the latter is the case, then in the study of Dela Pena and Roy [42], PP deposition resulted in a large fraction of ordered grain boundaries (the A value is even by 30% smaller than the reference value for average random grain boundaries), whereas DC plating (the A value is by a factor of 2 higher than the reference value for average random grain boundaries) resulted in a very large fraction of high-angle grain boundaries, the latter having a relatively high grain-boundary resistivity [43]. It may be worth to note that PP electrodeposition yielded in both Refs. [41] and [42] A(Cu) values smaller than the reference value.

Returning to the results presented in Fig. 5, we may say that the resistivities observed to be smaller than the reference data could be ascribed, based on the observation of Woo [41], to the presence of a relatively large fraction of more ordered grain boundaries exhibiting a correspondingly smaller contribution to the resistivity than the average (mainly more disordered) grain boundaries. This hints at the necessity of carrying out more detailed investigations in the future to what extent the preparation methods and preparation parameters can influence the degree of disorder of grain boundaries in the nano-sized grain regime since this also could give an important tool for reducing the resistivity of metallic conductors at small interconnect line dimensions.

There is one more report on the resistivity of Cu thin films with detailed grain size study and this deserves special attention to be discussed separately after the analysis of previous results. Chawla et al. [44] carried out a detailed analysis of the room-temperature resistivity of evaporated and subsequently annealed Cu films. These authors prepared 20-, 30- and 40-nm-thick films first and then the thicker films were thinned down by sputtering to have the same thickness for each of them. The grain size was established from EBSD analysis by evaluating 5000 to 10,000 grains for each sample. An XRD study revealed a strong (111) texture of the films. The resistivities were found to be higher in the samples of Chawla et al. [44] (see open symbols in Fig. 7) than in the films of Sun et al. [1] for comparable grain sizes (indicated by the thick line as reference data in Fig. 7). This means that there seems to be some additional resistivity contribution in the films of Chawla et al. [44] the magnitude of which varies from sample to sample. In addition to the film preparation methods (sputtering: Ref. [1]; evaporation: Ref. [44]), a distinct difference between the films of the two reports was that Sun et al. [1] deposited a SiO_2 or a SiO_2/Ta cap layer on top of the Cu films which must have been very effective to prevent any later oxidation of the Cu thin films. On the other hand, Chawla et al. [44] did not use a protecting cap layer and since they measured the resistivities at ambient condition, an oxide layer on top of the Cu films may have resulted in larger resistivities for comparable grain sizes than in the work of Sun et al. [1] due to surface specularity differences. Another particular feature of the procedure of Chawla et al. [44] was the thinning by sputtering which may also have changed the surface specularity, eventually even in a random manner, explaining the scatter of the excess resistivity values over the grain size range investigated.

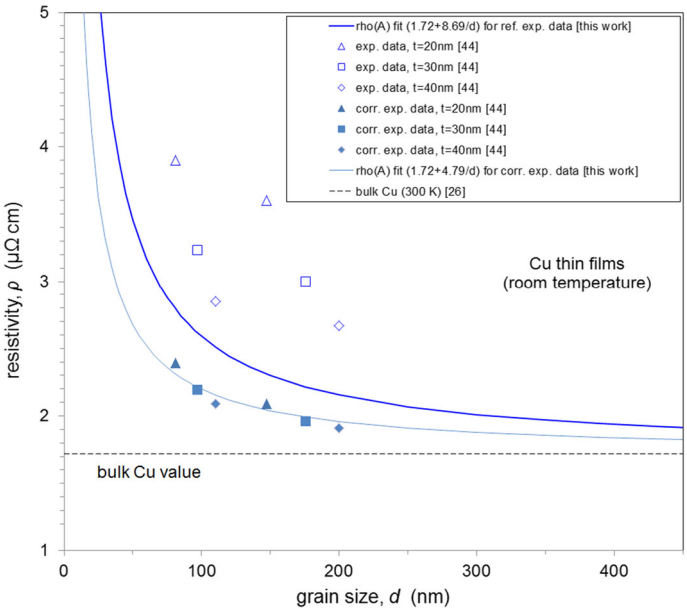

Fig. 7 Room-temperature resistivity ρ for Cu films as a function of the grain size d. The thick solid line represents a fit to Eq. (6) with fixed $\rho_{\text{bulk}} = 1.72\ \mu\Omega$ cm [26] and with fitted value $A = 8.69 \times 10^{-16}\ \Omega\text{m}^2$ for the reference $\rho_{\text{exp}}(d)$ data (T = 296 K) of Ref. [1]. The experimental data (T = 298 K) of Ref. [44] are indicated by the open triangle (original film thickness t = 20 nm), square (t = 30 nm) and diamond (t = 40 nm) symbols. The full symbols represent data of the same specimens after a correction as described in the text. The thin solid line represents a fit to Eq. (6) with fixed $\rho_{\text{bulk}} = 1.72\ \mu\Omega$ cm [26] and with fitted value $A = 4.79 \times 10^{-16}\ \Omega\text{m}^2$ to the corrected data of Ref. [44]

We can proceed with the data analysis if we take into account that, in order to separate thickness effects and differences in background resistivities, Chawla et al. [44] also investigated single-crystal (SC) Cu films which were produced with the same thickness and thinned in the same manner as the above discussed polycrystalline Cu films. Since the single-crystal films did not have any grain boundaries, their resistivity contains contributions only from the electron–phonon scattering as well as from surface scattering processes. Therefore, if we subtract for each sample with different original film thicknesses the difference $\rho(\text{SC}) - \rho_{\text{bulk}}$ (where $\rho_{\text{bulk}}(\text{Cu};300\ \text{K}) = 1.72\ \mu\Omega$ cm) from the measured resistivity of the corresponding polycrystalline film sample, then this value should reflect the grain-boundary contribution above the bulk resistivity. After this correction of the experimental data, we get the resistivities for the polycrystalline Cu films of Chawla et al. [44] which are displayed in Fig. 7 by the solid symbols.

These data all falling below the reference data (thick solid line) show a continuous decrease with increasing grain size and exhibit a very small scatter only. If we now perform an Andrews fit according to Eq. (6) for these corrected data, we get $A(\text{Cu}) = 4.79 \times 10^{-16}\ \Omega\text{m}^2$ by using the standard Cu bulk value $\rho_{\text{bulk}}(\text{Cu};300\ \text{K}) = 1.72\ \mu\Omega\text{cm}$. This low $A(\text{Cu})$ value in comparison with the corresponding value for the average random grain boundaries [$A(\text{Cu}) = 8.69 \times 10^{-16}\ \Omega\text{m}^2$] may indicate that in the evaporated thin Cu films studied by Chawla et al. [44] the fraction of more ordered grain boundaries, either due to the film preparation details or due to the applied subsequent annealing or both, was fairly large as was also the case for the Cu electrodeposits investigated by Woo [41]. It is recalled, furthermore, that the Cu films

studied by Chawla et al. [44] exhibited an almost perfect (111) texture as a consequence of which the distribution of types of grain boundaries perpendicular to the film plane is probably also not completely random and, in a favorable case, this may also lead to a reduced grain-boundary contribution to the resistivity. This specific study calls attention to the importance of studying more carefully thin film texture when analyzing the influence of grain boundaries on the resistivity in polycrystalline samples. We will return to the results of Chawla et al. [44] also in the next section when discussing the grain-boundary reflection coefficient results in the MS model for Cu metal.

In summary, we may say that a deviation of the reported grain-size dependence of resistivity from the reference $\rho_{\text{exp}}(d)$ data specified for polycrystalline Cu metal with random grain boundaries (and the corresponding difference in the Andrews parameter values) can be due to several reasons. A trivial source of error is if, although the experimental data can be well fitted by the Andrews method, the fit results in a lower ρ_{bulk} value than the standard bulk value $\rho_{\text{bulk}}(\text{Cu};300\ \text{K}) = 1.72\ \mu\Omega\text{cm}$ since this seems to indicate an improper calibration of the absolute value of the resistivity which can then be made, at least partially, responsible for the deduced lower A(Cu) value. If the fitted bulk resistivity is higher than the standard bulk value, it may be again due to an improper resistivity calibration or due to impurities. A predominance of grain boundaries with higher resistivity contribution may also lead to higher background resistivity and/or higher A(Cu) value. We could also see above on the example of the results from Ref. [27] that even if the experimental data could be fitted by the Andrews method with the standard bulk value $\rho_{\text{bulk}}(\text{Cu};300\ \text{K}) = 1.72\ \mu\Omega\ \text{cm}$, the A(Cu) value was still lower than our reference value for Cu metal with random grain boundaries. As discussed previously, this can be ascribed either to a preferential occurrence of special grain boundaries with more order than the average random grain boundaries or to the presence of a texture resulting predominantly in low-resistivity grain-boundaries in the path of the electrons carrying the current to measure the resistivity.

By finishing the analysis of the resistivity data for Cu by the Andrews method, it is noted that similarly to the case of nc-Ni, we will make an estimate of the maximum room-temperature resistivity also for nc-Cu in "Appendix C".

2.2.2 Cu resistivity data evaluated by the Mayadas–Shatzkes model

As discussed in Sect. 2.1.2 when evaluating resistivity data for Ni metal in the MS model, the electron mean free path λ decisively influences, via Eq. (10), the value of the grain-boundary reflection coefficient R derived from matching the calculated ρ_{MS} curves to the experimental data. Concerning the electron mean free path, the situation is much clearer for Cu than was for Ni. By using $\rho_{\text{bulk}}(\text{Cu},300\ \text{K}) = 1.72\ \mu\Omega\ \text{cm}$ [26], the free-electron estimate [31] and the theoretical calculation of Gall [5] yield $\lambda(\text{Cu},300\ \text{K}) = 38.1$ nm and 39.0 nm, respectively. Furthermore, there seems to be a general consensus [1, 5, 44, 45] that the experimental value is $\lambda(\text{Cu},300\ \text{K}) = 39.0$ nm and we will use this latter value in evaluating experimental Cu data with the MS model.

In spite of the well-defined value of the electron mean free path for Cu, there is still a large scatter of the reported R values ranging from 0.1 to 0.8 as summarized in Refs. [45] and [46]. Since R is usually determined from resistivity vs. thickness data obtained on thin films for which the evaluation should be based on a combination of the FS and MS models, the film surface specularity parameter therefore also enters the problem. Since different combinations of the specularity parameter and the reflection coefficient often yield an equally good fitting of the experimental data [2], this procedure may easily result in an erroneous R value.

In order to get rid of this problem, we should first concentrate on selecting reliable experimental data where, in addition, the surface scattering is negligible or very small and, thus, we can eliminate the uncertainty due to the choice of the specularity parameter.

It was demonstrated in the previous section that the experimental results of Sun et al. [1] can be considered as reference resistivity vs. grain size data for Cu metal with random grain boundaries. This is substantially supported by the fact that the low-temperature resistivity vs. grain size data of Ref. [1] match very well the corresponding data of Andrews et al. [35] on massive Cu specimens (at $T = 4.2$ K, the A(Cu) values from the two reports agree within about 12%) since for the latter case, there is no concern of the surface scattering effects. Therefore, we will start the discussion of the MS model evaluations with the data of Sun et al. [1].

By using the MS model for grain-boundary scattering according to Eqs. (8) to (10) and taking the usual value of $[\rho_{\rm bulk}\lambda_{\rm bulk}]_{\rm Cu} = 6.6 \times 10^{-16}$ Ωm^2, Sun et al. [1] deduced R(Cu;296 K) = 0.49 from their room-temperature experimental data (at $T = 4.2$ K, they obtained R(Cu;4.2 K) = 0.45). Their $\rho_{\rm exp}(d)$ data considered as the reference resistivity data for polycrystalline Cu metal with random grain boundaries are represented by the thick solid line in Fig. 8 which corresponds to an Andrews fit with A(Cu) $= 8.69 \times 10^{-16}$ Ωm^2. We have displayed a $\rho_{\rm MS}(d)$ function with R(Cu;296 K) = 0.475 (represented by the open circles) which shows the best agreement with the reference experimental data represented by the thick solid line and the value of R(Cu;296 K) = 0.475 is close to that of Sun et al. [1]. Two other $\rho_{\rm MS}(d)$ functions (thin solid lines with symbols) are also given to illustrate the evolution of these functions with increasing R values.

Sun et al. [1] performed a careful evaluation of their data by using also a combination of the FS and MS models and various extensions of them (the fit quality parameter was evaluated also in a manner as to account for the number of fitted parameters). Somewhat better fit quality was achieved in the extended models and the best R(Cu;296 K) value of 0.43 was obtained from three of these models which take into account some degree of surface scattering as well. Nevertheless, this value is not very different from the above R(Cu;296 K) = 0.49 value which was derived from the application of the MS model only to the experimental data and even this model led to a relatively high-quality fit. Our R(Cu;296 K) = 0.475 value for the same data also matches well the results of Sun et al. [1].

We will pay some attention again to the data of Andrews et al. [35] on a massive Cu specimen at $T = 4.2$ K which data were represented by the dash-dot line in Fig. 4. Due to the macroscopic size of their specimen, the problem of surface specularity does not enter the evaluation by the MS model since surface scattering can evidently be neglected here. Andrews et al. [35] found that the bulk resistivity in their Cu specimen was $\rho_{\rm bulk}$(Cu,4.2 K) = 0.00079 $\mu\Omega$ cm. By taking the calculated value of $[\rho_{\rm bulk}\lambda_{\rm bulk}]_{\rm Cu} = 6.7 \times 10^{-16}$ Ωm^2 [5], we get from this resistivity $\lambda_{\rm bulk}$(Cu,4.2 K) = 83,500 nm for the bulk Cu mean free path in their specimen at 4.2 K. Constructing $\rho_{\rm MS}(d)$ functions with this electron mean free path in the MS model, we find a perfect match with their experimental data by choosing R(Cu;4.2 K) = 0.49 for the grain-boundary reflection coefficient of Cu metal. This value matches fairly well the low-temperature result derived above from Cu thin film data of Sun et al. [1].

In conclusion, from the grain-size dependence of those resistivity data which we considered as reference data, a reflection coefficient of R(Cu) $= 0.46 \pm 0.03$ can be deduced for polycrystalline Cu metal with random grain boundaries. By considering the evolution of the $\rho_{\rm MS}(d)$ functions with R for a constant value of the electron mean free path λ as shown in Fig. 8, we can see that this behavior of R is very similar to that of the Andrews parameter A.

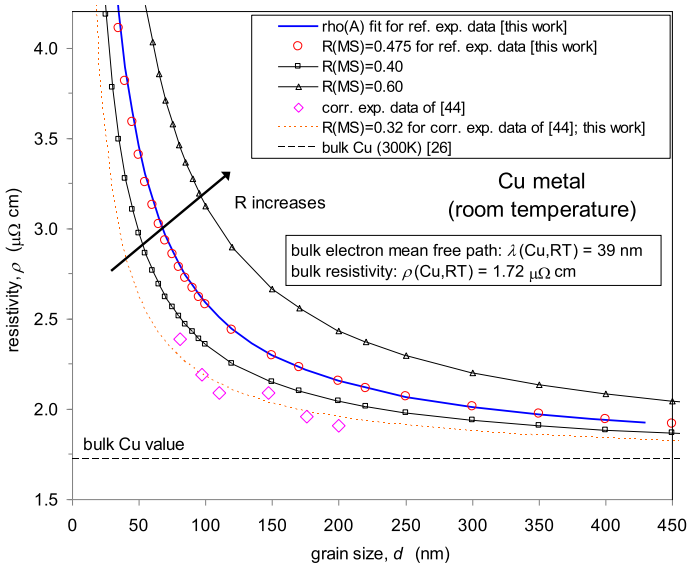

Fig. 8 Resistivity ρ at room temperature for Cu as a function of the grain size d. The thick solid line displays the reference experimental data which are represented by the Andrews fit according to Eq. (6) with parameters $\rho_{\text{bulk}} = 1.72\ \mu\Omega$ cm [26] and $A = 8.69 \times 10^{-16}\ \Omega\text{m}^2$. The open circles correspond to a calculated $\rho_{\text{MS}}(d)$ function according to Eq. (8) of the MS model [14] with $R = 0.475$ to best match the reference experimental data with the specified bulk electron mean free path (emfp) value. The two thin lines with symbols represent the calculated $\rho_{\text{MS}}(d)$ functions with R values as given in the legend. The arrow indicates the direction of the increase of R for a fixed emfp value. The diamond symbols display the corrected data of Ref. [44] as taken from Fig. 7 and the thin dashed line is the best-matching $\rho_{\text{MS}}(d)$ function with $R = 0.32$

This implies that if the experimental data are, for a given size, above or below the reference $\rho_{\text{exp}}(d)$ data, then both the R and A values will be usually larger or smaller than the value of these parameters derived here for the random grain boundaries of polycrystalline Cu metal. With reference to Figs. 5, 6, and 7, we have already seen in Sect. 2.2.1 that the reported resistivity values in several cases deviated, mostly towards lower resistivity values, from the reference $\rho_{\text{exp}}(d)$ data for Cu metal. This deviation was naturally accompanied by a reduced Andrews parameter value deduced from such data with respect to our reference value (A(Cu) $= 8.69 \times 10^{-16}\ \Omega\text{m}^2$). We will see now here below that the reported R(Cu) values of these reports were also correspondingly smaller than our preferred R(Cu) = 0.46 value as specified above.

Tochitskii and Belyavskii [27] reported an A(Cu,300 K) $= 3.90 \times 10^{-16}\ \Omega\text{m}^2$ value and their specified reflection coefficient deduced from the MS model according to Eqs. (8)–(10) by taking λ_{bulk}(Cu,300 K) = 39 nm was R(Cu) = 0.28. From the results of Artunc and Öztürk [37], we derived A(Cu,300 K) $= 6.10 \times 10^{-16}\ \Omega\text{m}^2$ and they reported R(Cu) = 0.38 for both as-deposited and annealed films in the same manner as in Ref. [27]. By applying the same method and using the same electron mean fee path, Bruschi et al. [38] obtained R(Cu) = 0.33 and Riedel et al. [39] obtained R(Cu) = 0.38; our corresponding deduced A(Cu) values from these data were $5.0 \times 10^{-16}\ \Omega\text{m}^2$ [38] and $5.8 \times 10^{-16}\ \Omega\text{m}^2$ [39], respectively. The situation is similar with the experimental data of Chawla et al. [44] who deduced R(Cu) = 0.25(5) and we derived A(Cu) $= 4.79 \times 10^{-16}\ \Omega\text{m}^2$. For the experimental data of Fenn et al. [36], we

have deduced $A(\mathrm{Cu}) = 8.77 \times 10^{-16}$ $\Omega\mathrm{m}^2$ and by using Dimmich's theory [47], these authors derived an average value of R = 0.35 for their films by taking $\lambda_{\mathrm{bulk}}(\mathrm{Cu},273\ \mathrm{K}) = 38.3$ nm.

We can see from the above listing that lower A(Cu) values are accompanied by lower R(Cu) values in these reported cases. In the case of the reported results of Wu et al. [40], the situation is the opposite, in that an $A(\mathrm{Cu}) = 9.7 \times 10^{-16}$ $\Omega\mathrm{m}^2$ value higher than the reference value [$A(\mathrm{Cu}) = 8.69 \times 10^{-16}$ $\Omega\mathrm{m}^2$] was derived by us for their data and, correspondingly, they obtained a fairly high reflection coefficient of about $R(\mathrm{Cu}) = 0.59$. We could analyze in the same manner also the results on electrodeposited Cu samples (see Fig. 6) although for these cases the bulk resistivity was fitted by the Andrews method to yield a higher value than the standard bulk value. Nevertheless, the deviation of the R(Cu) values in the above discussed reports from the reference R(Cu) value derived here for polycrystalline Cu metal with random grain boundaries can be explained in the same manner as we did for the A(Cu) values at the end of Sect. 2.2.1.

In a similar manner as for Ni (cf. Figure 3), we constructed a room-temperature R vs. λ plot also for Cu on the basis of the MS model and these data could be fitted with the relation $R = -0.2337 \cdot \ln(\lambda) + 1.3267$. By recalling that for Ni we obtained $R = -0.2344 \cdot \ln(\lambda) + 1.1212$, we can see that, not surprisingly, the coefficient of the logarithmic term for Cu is practically the same as for Ni.

As noted for Ni at the end of Sect. 2.1.2, reports on resistivity studies of Cu metal with solely XRD-based microstructural characterization will be discussed in "Appendix B".

3 Comparison of the Andrews parameter A and the reflection coefficient for Ni and Cu

3.1 Summary of A and R data for Ni and Cu as derived in the present work

It could be shown in Sect. 2 that a given experimental data set of resistivity vs. grain size can be fitted both with the MS model [14] and the Andrews method [15]. We have derived the Andrews parameter A (Andrews method) and the reflection coefficient R (MS model) for Ni and Cu which are considered as quantities characterizing the grain-boundary resistivity contribution in polycrystalline Ni and Cu metals with random grain boundaries. The best A values deduced in the present paper from those experimental $\rho_{\mathrm{exp}}(d)$ results which were considered as reference data for these metals are as follows: $A(\mathrm{Ni};300\ \mathrm{K}) = 14.7 \times 10^{-16}$ $\Omega\mathrm{m}^2$ and $A(\mathrm{Cu};300\ \mathrm{K}) = 8.69 \times 10^{-16}$ $\Omega\mathrm{m}^2$.

As discussed in "Appendix A.1", the Andrews parameter A is a reliable experimental quantity, being independent of any model assumption provided the measured resistivities scale linearly with the inverse of the grain size as first observed by Andrews [15] and demonstrated in Sect. 2 with results from many studies on both Ni and Cu metals. On the other hand, the reflection coefficient R introduced in the MS model [14] is dependent, in addition to the validity of the model assumptions, also on the electron mean free path at the temperature of the measurement as discussed in "Appendix A.2".

In Table 1, we have listed the room-temperature values of R for Ni and Cu both as obtained from a direct fit of the MS model to the reference $\rho_{\mathrm{exp}}(d)$ data in previous sections and as derived from Eq. (15) by using the above determined A(Ni) and A(Cu) values. It should be noted that whereas there is a consensus in the literature about the electron mean free path of bulk Cu as $\lambda_{\mathrm{bulk}}(\mathrm{Cu};300\ \mathrm{K}) = 39$ nm [5] since the experimental and theoretical values agree within a few percent, the reported theoretical ($\lambda_{\mathrm{bulk}}(\mathrm{Ni};300\ \mathrm{K}) = 5.62$ nm [5]) and experimental ($\lambda_{\mathrm{bulk}}(\mathrm{Ni};300\ \mathrm{K}) = 26$ nm [32]) values are widely different for Ni. Therefore, we provide the R(Ni) values in Table 1 for both above electron mean free path values of Ni.

Table 1 Grain-boundary reflection coefficient R of the MS model [14] derived with λ_{bulk} values as specified for Ni and Cu metals either by a direct $\rho_{MS}(d)$ fit to the reference room-temperature $\rho_{exp}(d)$ data or with the help of Eq. (15) by using ρ_{bulk}(Ni,300 K) = 7.24 μΩ cm [26] and ρ_{bulk}(Cu,300 K) = 1.72 μΩ cm [26]

Metal	Grain-boundary reflection coefficient R	R source	Condition for α <<1 (α <0.1)
Ni	$R = 0.717$	$\rho_{MS}(d)$ fit to reference $\rho_{exp}(d)$ data with A(Ni;300 K) = 14.7×10^{-16} Ωm^2 and with theoretical λ_{bulk}(Ni;300 K) = 5.62 nm [5]	n.a
	$R = 0.707$	From Eq. (15) with A(Ni;300 K) = 14.7×10^{-16} Ωm^2 and with theoretical λ_{bulk}(Ni;300 K) = 5.62 nm [5]	α <0.1 if d >135 nm
Ni	$R = 0.355$	$\rho_{MS}(d)$ fit to reference $\rho_{exp}(d)$ data with A(Ni;300 K) = 14.7×10^{-16} Ωm^2 and with experimental λ_{bulk}(Ni;300 K) = 26 nm [32]	n.a
	$R = 0.342$	From Eq. (15) with A(Ni;300 K) = 14.7×10^{-16} Ωm^2 and with experimental λ_{bulk}(Ni;300 K) = 26 nm [5]	α <0.1 if d >135 nm
Cu	$R = 0.475$	$\rho_{MS}(d)$ fit to reference $\rho_{exp}(d)$ data with A(Ni;300 K) = 8.69×10^{-16} Ωm^2 and with λ_{bulk}(Cu;300 K) = 39 nm [5]	n.a
	$R = 0.463$	From Eq. (15) with A(Cu;300 K) = 8.69×10^{-16} Ωm^2 and with λ_{bulk}(Cu;300 K) = 39 nm [5]	α <0.1 if d >335 nm

The application of Eq. (15) is valid only in the limit of $\alpha = (\lambda_{bulk}/d)[R/(1–R)] << 1$.
n.a. = not applicable

Table 1 reveals that, for a given value of the electron mean free path, the reflection coefficient values derived by the two methods agree fairly well with each other for both metals.

3.2 Discussion of the magnitude of the grain-boundary resistivity parameters A and R

3.2.1 Grain-boundary resistivity parameters A and R for Cu metal

We start the discussion with Cu for which the electron mean free path has a well-defined standard value (λ_{bulk}(Cu;300 K) = 39 nm [5]). As demonstrated in Sect. 2.2.1, the reliable Andrews parameter for polycrystalline Cu metal with random grain boundaries is A(Cu;300 K) = 8.69×10^{-16} Ωm^2 which could be converted to $R = 0.463$ with this mean free path value by using Eq. (15). By carrying out a matching of $\rho_{MS}(d)$ functions (MS fit) to the average experimental resistivity vs. grain size data of Sun et al. [1], we derived R = 0.475 which value agrees well with $R = 0.49$ as obtained with the MS model by Sun et al. [1] for their data. These latter authors have carried out a detailed fitting by extending the MS model in various ways by taking into account surface scattering and surface roughness effects as well. They came to the conclusion that the best fit was obtained when the combined MS and FS fit was applied which yielded $R = 0.43$ for the reflection coefficient. By taking all these circumstances into account, we suggest herewith that the current best value for the

reflection coefficient of Cu is $R(\text{Cu};300\ \text{K}) = 0.46 \pm 0.03$ which uncertainty range covers all above specified R values.

3.2.2 Grain-boundary resistivity parameters A and R for Ni metal

A well-defined experimental value of $A(\text{Ni};300\ \text{K}) = 14.7 \times 10^{-16}\ \Omega\text{m}^2$ was derived above for polycrystalline Ni metal with random grain boundaries. Due to the fact that there is a large difference between the theoretical and experimental electron mean free paths for Ni metal, we could derive, both by a direct MS fitting to the experimental data and by using Eq. (15), two values (ca. 0.35 and ca. 0.7, respectively) for $R(\text{Ni})$ as can be seen in Table 1 which values differ roughly by a factor of 2. The real bulk electron mean free path for Ni is expected to lie somewhere between the theoretical and experimental values, but at the moment we cannot make any definitive statement about it. Therefore, we can only say that the real value of $R(\text{Ni})$ is possibly in the range from 0.35 to 0.70.

3.2.3 Comparison of the grain-boundary Andrews parameter A for Ni and Cu metals

As far as the above derived values of the Andrews parameters $A(\text{Ni};300\ \text{K}) = 14.7 \times 10^{-16}\ \Omega\text{m}^2$ and $A(\text{Cu};300\ \text{K}) = 8.69 \times 10^{-16}\ \Omega\text{m}^2$ are concerned, there is no doubt that they correctly describe the measured $\rho_{\text{exp}}(d)$ data for the two metals without any model assumptions. These data imply that $A(\text{Ni}) = 1.7\ A(\text{Cu})$ which qualitatively corresponds to expectation in that Ni is considered as a "more resistive" metal than Cu on the basis of their bulk resistivities [26]: $\rho_{\text{bulk}}(\text{Ni},300\ \text{K}) = 7.24\ \mu\Omega\ \text{cm}$ and $\rho_{\text{bulk}}(\text{Cu},300\ \text{K}) = 1.72\ \mu\Omega\ \text{cm}$. However, we can also see that $\rho_{\text{bulk}}(\text{Ni},300\ \text{K}) = 4.2\ \rho_{\text{bulk}}(\text{Cu},300\ \text{K})$ which is larger by more than a factor of 2 in comparison with the ratio of the Andrews parameters of these metals.

We may perhaps proceed also along another route of thinking. According to Eq. (5), A is proportional to ρ_{SGBR}, the specific grain-boundary resistivity which is the resistivity contribution per unit grain-boundary area when a grain boundary is considered as a resistive wall of finite thickness with a well-defined resistivity per surface area. In this sense, the Andrews parameter A is a measure of the specific resistivity of the grain boundary as a wall through which the electron should pass along its way towards the lower electric potential. (Of course, the value of parameter A derived from measurements on polycrystalline specimens represents a mean value of the grain-boundary resistivities averaged over different types of grain boundaries and over different relative orientations of the grain-boundary plains with respect to the electron trajectory.) Both Ni and Cu metals have an fcc crystal structure, so we may assume in a first approximation that they have the same degree of atomic disorder in the grain boundaries. This disorder is the basic source of excess resistivity due to the presence of grain boundaries beyond the background resistivity within the crystallites (ρ_{bulk}). As we discuss in "Appendix C", the structural disorder from the perfect crystal to the structurally disordered (amorphous) state induces roughly the same amplification of the resistivity at 300 K for Ni and Cu (by a factor of 9.7 and 7.1, respectively). Therefore, the difference in the $A(\text{Ni})$ and $A(\text{Cu})$ values cannot be ascribed to structural differences, but rather to the different resistivities of the two metals and this can be rationalized in the following manner.

The different resistivities of Ni and Cu can be understood by the model of Mott [48] who realized that transition metals like Ni have a large d-band density of states at the Fermi level, whereas noble metals have only s-electron density of states at the Fermi level. The resistivity can be considered as being proportional to the scattering probability of the current-carrying conduction electrons (mainly s-electrons). In other words, the resistivity arises from

scattering of electrons on any obstacles along the electron pathways. According to Fermi's "golden rule" as formulated by Rossiter [49], the scattering probability depends not only on the matrix element of the scattering potential between the initial and final electron states, but it is also proportional to the total electronic density of states at the Fermi level. This latter condition arises because electrons at the Fermi energy only can participate in the conduction process and they can be scattered to energy states only in the immediate vicinity of the Fermi level; therefore, the probability of scattering should depend on the amount of vacant states which are available to accept electrons after scattering. The high d-band density of states in Ni explains [48] the higher resistivity of Ni in comparison with Cu at a given temperature, quantitatively given by the relation $\rho_{\text{bulk}}(\text{Ni,300 K}) = 4.2\ \rho_{\text{bulk}}(\text{Cu,300 K})$.

We may try in the same picture to rationalize also the fact that we have found above experimentally for the Andrews parameters of the two metals the relation $A(\text{Ni}) = 1.7\ A(\text{Cu})$. Since A was above identified as characterizing the resistivity of the grain boundary as a resistive wall, this means that the grain-boundary (wall) resistivity is not so "efficient" in Ni than in Cu, at least in comparison with their bulk resistivities in the perfect crystalline state (bulk). On the other hand, it is usually known that any distortion of the crystal lattice and/or reduction of the nearest-neighbor numbers may lead to a broadening of the peaks of the density of states and this broadening can be expected to result in a decrease of the d-band density of states at the Fermi level. Since these effects due to the inherent disorder may evidently occur in the grain boundaries, they naturally lead to a reduction of the vacant states available for the scattered electrons in Ni and thus the resistivity of grain boundary may less effectively increase in the grain boundaries in Ni than in Cu, the latter having practically no d-band density at the Fermi level. We should also recall that the topological disorder in the grain boundaries is expected to be the same for the two metals due to their common fcc structure.

If the above reasoning prevails, we could explain why the ratio of the Andrews parameters of Ni and Cu is smaller (1.7) than the ratio of their room-temperature bulk resistivities (4.2). Since according to Eq. (5) the specific grain-boundary resistivity ρ_{SGBR} is proportional to the Andrews parameter A, the ratios of both quantities are identical for the two metals (since the proportionality factor k_{GB} is a topology-dependent quantity). All these considerations based on the experimental data for the two selected metals (Ni and Cu) also imply that the resistivity increment due to the presence of grain boundaries is not directly proportional to the bulk resistivity although a larger ρ_{bulk} seems to result in larger A and ρ_{SGBR} values.

It may be appropriate at this point to summarize in some way the essence of the Andrews approach for evaluating a grain-boundary resistivity parameter. It is important to emphasize that no model assumptions were necessary in setting up the formulas in Eqs. (1) to (6) of "Appendix A", these equations simply correspond to the experimental observation in that the variation of the resistivity of a metal can be described as the sum of a bulk resistivity and a term due to the presence of grain boundaries which is proportional to the inverse of the mean grain diameter d. As discussed in "Appendix A.1", stereological considerations suggest that the grain-boundary surface area per unit volume (S_{GB}/V) is proportional to $1/d$, the quantity S_{GB}/V is also proportional to the total resistivity contribution by the grain boundaries. This is expressed by Eq. (2) which immediately defines ρ_{SGBR}, the specific grain-boundary resistivity which represents the resistivity increment due to the grain-boundary surface area per unit volume. All in one, both A and ρ_{SGBR} are a measure of the specific resistivity contribution of grain boundaries. In this sense, we may consider a polycrystalline specimen as consisting of a bulk material component characterized by ρ_{bulk} which component is connected in series with a grain-boundary component ρ_{GB} which is characterized by ρ_{SGBR}. The smaller the

grain size, the larger the amount of grain boundaries in the specimen and this leads then to a larger ρ_{GB}, whereas the contribution ρ_{bulk} remains unchanged with varying grain size.

In this phenomenological type of description of the experimental results, the strongly temperature-dependent electron mean free path does not enter the picture and, therefore, we may not expect a significant temperature dependence of the Andrews parameter A. In a simple picture, the Andrews parameter A measures the strength of the hindrance of electron flow through a grain boundary whereby the topological disorder of the grain boundary is mainly responsible for this hindrance. However, whereas this topological disorder is static at low temperatures (liquid helium temperature range), it may exhibit a dynamic component as well at elevated temperatures due to the excitation of phonons. Therefore, a small increase of A with increasing temperature would be physically realistic although it would be hard to predict the degree of this temperature dependence. In any case, the weak but still measurable temperature dependence of A reported for both Ni an Cu metals in several cases (about 20%, from 4.2 K to 300 K, see Sects. 2.1.1 and 2.2.1 as well as "Appendix B") could be explained with the previously described picture.

The physical reality of the picture about the grain-boundary contribution to the resistivity, i.e., that we can assign a definite resistivity value to a grain boundary as a wall of finite thickness was first evidenced by the delicate efforts of Nakamichi [43] who was able to measure the resistivity contribution of a single grain boundary.

Nakamichi [43] investigated the resistivity of small strip-shaped bicrystals containing a single grain boundary of various known orientations by measuring the resistivity increment over the bulk resistivity in a segment of the strip which contained one grain boundary only. The large cross-Sect. ($1 \times 3\,mm^2$) of the high-purity Al specimen (99.9999%, RRR = 30,000) ensured that, in spite of the long mean free path (ca. 500 Ωm) at 4.2 K, the surface scattering effects still remained negligible. The specific grain-boundary resistivity was mapped out for various grain boundary types as defined by their tilt and twist angles. An important outcome of this work was that the results obtained lend themselves to a picture that the grain-boundary resistivity arises from the electron scattering by the dislocations constructing the grain boundary. The conclusions in general are, of course, valid for other metals as well.

3.2.4 Comparison of the grain-boundary reflection coefficient R for Ni and Cu metals

We should start discussion by noting that the grain-boundary reflection coefficient is a natural ingredient in the Mayadas–Shatzkes model [14] in which the Boltzmann equation was solved in the relaxation time approximation. The relaxation time is defined as the average time between two scattering events of an electron and it is directly related to the electron mean free path which is the average distance traveled by the electron between two scattering events. The solution of the Boltzmann equation was found [14] in a specific form in which only the ratio of the mean free path and the average distance between the locations of the grain boundaries as scattering walls appeared (see Eq. (10) in "Appendix A"). The average distance between the locations of the grain boundaries was then identified as the mean grain diameter [14]. In the MS model [14], the grain boundaries are considered as planes characterized by a potential on which the electrons can be scattered and a scattering results either in a reflection or a transmission of the electron impinging on the potential wall. Evidently, a resistivity contribution arises which is proportional to the probability of the electron reflection characterized by the reflection coefficient R. Evidently, R is a monotonically increasing function of the grain-boundary scattering potential. In this manner, the reflection coefficient R which contains information on the scattering potential of the grain boundaries should also appear in the resistivity term characterizing the grain-boundary contribution [c.f. in Eqs.

(8) to (10)]. The total resistivity formula in the MS model, $\rho_{MS}(d)$, indeed results in larger resistivity for larger R as is demonstrated in Figs. 2, 3, 4, 5, 6, 7, and 8.

As discussed above, we could derive for Cu a well-defined value for the grain-boundary reflection coefficient: $R(\text{Cu};300\text{ K}) = 0.46 \pm 0.03$. On the other hand, it was found that the possible range of R(Ni) extends from 0.35 to 0.7. Intuitively, we may expect that the scattering potential of a grain boundary is larger in Ni than Cu. Therefore, the first expectation is that the relation $R(\text{Ni}) > R(\text{Cu})$ should hold. This would imply that the possible real R(Ni) value should be between about 0.5 and 0.7.

Nevertheless, it can be revealed from Figs. 2, 3, 4, 5, 6, 7, and 8 that for a given metal, the larger the Andrews parameter A as derived via Eq. (6) from the $\rho_{exp}(d)$ data, the larger reflection coefficient results from the $\rho_{MS}(d)$ fit to the same data set. Therefore, we should expect that if one metal (M_1) has a larger A value than another metal (M_2), the same should hold for their R values as well, i.e., if $A(M_1) > A(M_2)$, then $R(M_1) > R(M_2)$ holds. This is not surprising actually since both parameters are thought of as a quantity characterizing the strength of the hindrance of electron motion through the grain boundary.

In the previous section, we attempted to rationalize the difference in the relations $\rho_{bulk}(\text{Ni},300\text{ K}) = 4.2\ \rho_{bulk}(\text{Cu},300\text{ K})$ and $A(\text{Ni}) = 1.7\ A(\text{Cu})$. The smaller proportionality factor in the second relation tells us that the same type of grain boundary in Cu provides a larger contribution to the resistivity than it would expected on the basis of the bulk resistivity of Ni and Cu. There have been recently some theoretical efforts [3, 50] that provide some further microscopic background which help us understand this apparent discrepancy in addition to the arguments given in the previous section on the basis of the different electronic density of states at the Fermi level for the two metals. It turned out namely [50] that due to the much smaller bulk modulus of Cu than that of Ni, there is an excess free volume in the grain boundaries of Cu with respect to the same grain boundary type of Ni. This excess free volume is associated with a larger energy density in the grain boundaries of Cu [50]. On the other hand, it was also demonstrated [3] that a larger energy density in the grain boundary results in a larger resistivity contribution by the given grain boundary. One may perhaps formulate all this also in a manner that the excess free volume causes a larger disorder in the grain boundary of Cu since the excess free volume is distributed over a larger distance on both sides of the grain boundary due to the smaller bulk modulus, i.e., weaker bonds. Therefore, a given type of grain boundary in Cu represents a larger topological disorder from the viewpoint of electrical transport than in Ni.

4 Comparison of experimental and theoretical data on the grain-boundary resistivity contribution for Ni and Cu metals

4.1 Experimental A and ρ_{SGBR} data for Ni and Cu

In Sect. 2, we have analyzed available electrical resistivity vs. grain size data reported in the literature for Ni and Cu metals. Our guiding principle was to reconstruct, if not explicitly given, the $\rho_{exp}(d)$ data from the provided derived parameters (Andrews parameter A, specific grain-boundary resistivity ρ_{SGBR} or grain-boundary reflection coefficient R) and then to compare them with each other as well as to check the reported data for reliability, confidence and conformity with other relevant data. On this basis, we have established the resistivity vs. grain size data sets which were considered as reference data and from these, we have derived the current best room-temperature values of the Andrews parameter A and reflection coefficient R for Ni and Cu metals which are summarized in Table 1. As already mentioned,

Table 2 Specific grain-boundary resistivity ρ_{SGBR} data from room-temperature experiments for Ni and Cu

Metal	Experimental parameter A (10^{-16} Ωm^2)	Experimental parameter ρ_{SBGR} (10^{-16} Ωm^2)
Ni (pc)	14.7 [this work]	4.5 to 6.2 (derived from A)
Cu (pc)	8.7 [this work]	2.7 to 3.7 (derived from A)
Cu	–	19.0, 23.3 and 25.9 [51] (directly measured on three different single random grain boundaries)
Cu	–	20 to 29 [52] (directly measured on several single random grain boundaries)
Cu	–	1.06(10) [53] (average of directly measured values on seven different single incoherent $\Sigma 3$ {211} grain boundaries)

The Andrews parameter A (cf. Table 1) was obtained from resistivity data on polycrystalline (pc) Ni and Cu specimens with random grain boundaries. Equation (5) $A = k_{GB}\ \rho_{SGBR}$ was used to convert A to ρ_{SGBR} (the range given for ρ_{SGBR} corresponds to the possible range of the proportionality constant $2.37 < k_{GB} < 3.24$, see "Appendix A.1). The last three rows provide the results of direct measurements of ρ_{SGBR} on single grain boundaries

since the $\rho_{exp}(d)$ data were obtained on polycrystalline specimens, these parameters are average values over all possible grain boundary types and orientations, i.e., they represent data for random grain boundaries. As discussed in Sect. 3, these average A and R values are well defined for Cu and also the A value for Ni, but there is some ambiguity with the value of R for Ni due to the widely different mean free path values derived from theory and experiment for this metal [5].

In theoretical approaches to account for the grain-boundary contribution to the resistivity of a metal, the calculated results are mostly given in the form of the specific grain-boundary resistivity ρ_{SGBR}. According to Eq. (5), we have the relation $A = k_{GB}\ \rho_{SGBR}$, so in principle it is straightforward to convert the experimentally derived A values into specific grain-boundary resistivity data. However, the proportionality factor k_{GB} as defined in Eq. (3) may have different values depending on the particular stereological model used to calculate the relation between the grain-boundary surface area per unit volume and mean grain diameter. As discussed in "Appendix A.1", in previous studies various values in the range $2.37 < k_{GB} < 3.24$ were used for the proportionality factor. When converting A to ρ_{SGBR} for a comparison of experiment and theory, we will also use these two extreme values to provide the best possible range of ρ_{SGBR} for Ni and Cu. In Table 2, we provide the average experimental value of A and ρ_{SGBR} for Ni and Cu metals obtained on polycrystalline specimens as described above.

In addition, there are results on the resistivity of single grain boundaries in Cu and these data are also included in Table 2. Kim et al. [51] determined ρ_{SGBR}(Cu;300 K) of single grain boundaries in a four-pin scanning tunneling microscope (STM) with finely spaced contact pins via measuring the resistance as a function of the position of the voltage-contact pin over microfabricated Cu nanowires of rectangular cross section with widths and thicknesses of several hundreds of nanometers. The Cu nanowires contained several grain boundaries extending through the whole cross section of the wire. The grain boundary types were identified with the help of EBSD maps showing the crystallographic orientations of the individual grains. From the discrete resistance jumps when the voltage-detection pin passed a grain boundary, the authors deduced ρ_{SGBR}(Cu;300 K) values for three different high-angle random grain boundaries. Kitaoka et al. [52] also observed a discrete resistance jump when passing through a grain boundary in a similar experimental arrangement, but they have not

reported any ρ_{SGBR} values. However, the experimental results of Kitaoka et al. [52] were re-evaluated by Kim et al. [51] to yield ρ_{SGBR}(Cu;300 K) values in agreement with their own results and the data of both studies are included in Table 2.

We can see that the ρ_{SGBR}(Cu;300 K) values reported in the latter studies [51, 52] from measurements on single random grain boundaries are larger by nearly an order of magnitude than the experimental value deduced from measurements on polycrystalline Cu as given in the second row of Table 2. There is no explanation at the moment why the experimental ρ_{SGBR}(Cu) values obtained in the studies on individual high-angle grain boundaries [51, 52] are much larger than the reference specific grain-boundary resistivity value (Table 2) as deduced in the present work from the average A(Cu) value based on the results of several studies for polycrystalline samples with random grain boundaries. Kim et al. [51] discussed the possible role of impurities which are very prone to accumulate at grain boundaries and may eventually lead to higher ρ_{SGBR} values; however, they have not found any direct evidence for an increased impurity concentration in the grain boundaries in their samples.

There may be a concern, however, that these very large ρ_{SGBR} values [51, 52] measured on single random grain boundaries do not correspond to the real specific resistivity of random grain boundaries if we consider the corresponding results of Nakamichi [43] on single grain boundaries of very high purity Al metal. Namely, Nakamichi [43] found that the typical ρ_{SGBR}(Al) values for various single random grain boundaries were scattered in the range 3 to 5×10^{-16} Ωm^2. These data are not very much different from the range 2×10^{-16} $\Omega m^2 < \rho_{SGBR}(Al) < 3.0 \times 10^{-16}$ Ωm^2 that we can derive from the measured grain-size dependence of resistivity which were reported on polycrystalline Al bulk [35] and thin film [27] specimens. There is no reason to believe that if the ρ_{SGBR} data measured on single random grain-boundaries and on polycrystalline samples with random grain boundaries match each other so well for Al, they could be different by nearly an order of magnitude for Cu since both metals have the same fcc structure and their room-temperature resistivities differ by 50% only. It should be noted, furthermore, that the Cu nanowires investigated in Refs. [51] and [52] were prepared by electrodeposition as in Ref. [40] and we should recall the discussion in connection with Fig. 6 where we could see that significant differences (by a factor of 6) were found in the values of the Andrews parameters for the various electrodeposited Cu samples and the apparently too large grain-boundary resistivities reported in Refs. [51] and [52] may be connected with the preparation method.

In a very recent paper, Bishara et al. [53] reported on a new experimental setup for measuring the resistivity of single grain boundaries with the help of four independent micromanipulator tips inside a scanning electron microscope. By FIB milling, narrow wires with 600 nm width and typically 50 mm length were cut from sputtered high-purity Cu films with a thickness of 500 nm on an insulating substrate and the grain boundaries were located and identified by EBSD in the wires. By arranging the four micromanipulator tips along a line over the wire, they could detect a discrete resistance jump when passing with the mobile voltage tip over a grain boundary. By averaging over seven measurements in different wires, they obtained a grain-boundary resistivity value $\rho_{SGBR} = 1.06(10) \times 10^{-16}$ Ωm^2 for the incoherent $\Sigma 3$ {211} grain boundary. In view of the $<\rho_{SGBR}(Cu)> \sim 3 \times 10^{-16}$ Ωm^2 value for average random grain boundaries (see Table 2), the result of Bishara et al. [53] is very reasonable (we will later compare it also to available theoretical values).

Table 3 Specific grain-boundary resistivity ρ_{SBGR} for random grain boundaries from theoretical calculations for Ni and Cu metals

Metal	Theoretical specific grain-boundary resistivity, ρ_{SBGR} (10^{-16} Ωm^2)			
	Brown [54]	Karolik and Luhvich [55]	Valencia et al. [56]	Kim et al [51]
Ni	1.9	6.2 (low-angle: 1.5 high-angle: 7.6)	–	–
Cu	2.2	2.1 (low-angle: 0.5 high-angle: 2.5)	ca. 5.5 ± 1 (random single grain boundaries)	13 (random single grain boundaries)

It is noted that the value from Ref. [51] was obtained from a free-electron estimate

4.2 Theoretical ρ_{SGBR} data for Ni and Cu

4.2.1 Calculations for random grain boundaries

For the theoretical treatment of the contribution of general random grain boundaries to the resistivity, we will first refer to the results of Brown [54] and Karolik and Luhvich [55]. Brown [54] calculated the grain-boundary resistivity under the assumption that the scattering is primarily due to the core of dislocations which constitute these grain boundaries. The later experimental conclusions of Nakamichi [43] give some support for this approach. In this treatment, Brown [54] first calculated the dislocation resistivities and then the dislocation densities in various grain boundaries, from which data the grain-boundary resistivity was then derived.

Karolik and Luhvich [55] started first from the same approach, but they have noticed that the dislocation description of grain boundaries is correct only for low-angle grain boundaries (tilt angle $< 15^o$–20°). In the high-angle region, the dislocation cores are converted into cylindrical pores and, therefore, the dislocation description of large-angle grain boundaries by Brown [54] may not be valid. Therefore, Karolik and Luhvich [55] applied the dislocation model for the low-angle grain boundaries and elaborated a model for treating the resistivity contribution of the more porous high-angle grain boundaries. So they have separately calculated the specific grain-boundary resistivity for both low-angle and high-angle grain boundaries and then calculating a mean value for a random polycrystalline specimen by properly averaging over all possible grain-boundary angles. From their reported calculated values, we can see that the average values were obtained approximately as $<\rho_{SGBR}> = 0.161 <\rho_{SGBR}>_{low\text{-}angle} + 0.805 <\rho_{SGBR}>_{high\text{-}angle}$.

The calculated ρ_{SGBR} values from these studies [54, 55] are given in Table 3. By comparing them with the experimentally deduced ρ_{SGBR} values (Table 2), we can see that the approach of Brown [54] strongly underestimates the experimental ρ_{SGBR}(Ni) value, whereas the theoretical result of Karolik and Luhvich [55] for Ni is just at the upper limit of the experimentally derived range set by the uncertainty of k_{GB}. On the other hand, the two theoretical values for Cu [54, 55] are close to each other, whereas both theoretical values are somewhat below the possible range of the experimental ρ_{SGBR}(Cu) value.

More recently, Valencia et al. [56] have carried out first-principles calculations with various methods for random single grain boundaries in Cu. As Table 3 shows, their ρ_{SGBR} values are larger by about a factor of 2 than the experimental values obtained for polycrystalline samples as well as the results of early calculations [54, 55] on random grain boundaries. On the other hand, they are also much lower (by about a factor of 5) than the experimental results [51, 52] measured on single random grain boundaries. It is noted that Kim et al. [51] has made a free-electron estimate for random grain boundaries in Cu metal and obtained a higher value than that of Valencia et al. [56] (see Table 3). At the moment, we cannot comment more on these discrepancies in the measured and calculated values.

4.2.2 Calculations for coincidence-site lattice type single grain boundaries

Although the theoretical calculation of ρ_{SGBR} for random grain boundaries is still apparently a challenging task, there is some progress for interfaces that can be described by coincident-site lattice (CSL) models which are characterized by the parameter ΣN where a larger value of N implies a higher complexity of the grain boundary [3, 57]. The simplest case is the coherent twin boundary ($\Sigma 3$) for which several calculations have been carried out and the results for Cu are in fairly good agreement with each other as demonstrated in Fig. 9 where we can also see that the calculated values for the coherent $\Sigma 3$ boundary match well the experimental value ($\rho_{SGBR}(Cu) = 0.17 \times 10^{-16}$ Ωm^2 [58]). We have included here the very recent result ($\rho_{SGBR}(Cu) = 1.06(10) \times 10^{-16}$ Ωm^2) of Bishara et al. [53] obtained by averaging data measured for seven single incoherent $\Sigma 3$ boundaries in Cu. This value is significantly larger (by about a factor of 5) than the reported theoretical and experimental data for the coherent $\Sigma 3$ boundary which is certainly mainly due to the much larger atomic disorder in an incoherent $\Sigma 3$ boundary with respect to the coherent counterpart.

There have been further reports on the theoretical calculations of $\rho_{SGBR}(Cu)$ also for more complex CSL boundary types and the results are summarized in Fig. 9 which show that the ρ_{SGBR} values are mostly scattered between about 1.5 and 2.5×10^{-16} Ωm^2, although with a monotonically increasing trend. The results of these first-principles based calculations for single CSL grain boundaries are, especially for higher ΣN values, fairly close, except for $\Sigma 11$ boundaries, to the theoretical values for Cu obtained by Brown [54] as well as by Karolik and Luhvich [55] for random distribution of grain boundaries which are shown in Table 3. However, they are still well below the range (2.7×10^{-16} $\Omega m^2 < \rho_{SGBR}(Cu) < 3.7 \times 10^{-16}$ Ωm^2) deduced from measured resistivity data on polycrystalline Cu specimens with random grain boundaries. It is noted, with reference to the discussion at the end of Sect. 3.2.4, that the exceptionally low resistivity of the $\Sigma 11$ boundaries could be explained [3] with the low interfacial energy of this specific grain boundary due to its highly symmetric character.

Dixit et al. [61] have made first-principles calculations of $\rho_{SGBR}(Cu)$ for several symmetric tilt grain boundaries (from $\Sigma 3$ to $\Sigma 73$) with various grain-boundary planes and tilt angles from 13° to 86°. For these symmetric tilt boundaries, the obtained results were all about $\rho_{SGBR}(Cu) = 1.0(5) \times 10^{-16}$ Ωm^2 which values are just intermediate between the calculated results shown in Fig. 9 for the coherent twin boundary ($\Sigma 3$) and for the grain boundaries with higher ΣN values. These authors have also calculated the specific grain-boundary resistivity for a non-twin grain boundary with (111)/(110) interface and obtained $\rho_{SGBR}(Cu) = 2.5 \times 10^{-16}$ Ωm^2 which is close to the highest values shown in Fig. 9.

It should also be noted in this context that according to the calculations of Lee et al. [60] for several non-symmetric CSL type ΣN boundaries, $\rho_{SGBR}(Cu)$ can have very high values in specific transport directions with respect to the crystal axes. This underlines again the importance of texture investigations of samples from which grain-boundary resistivity

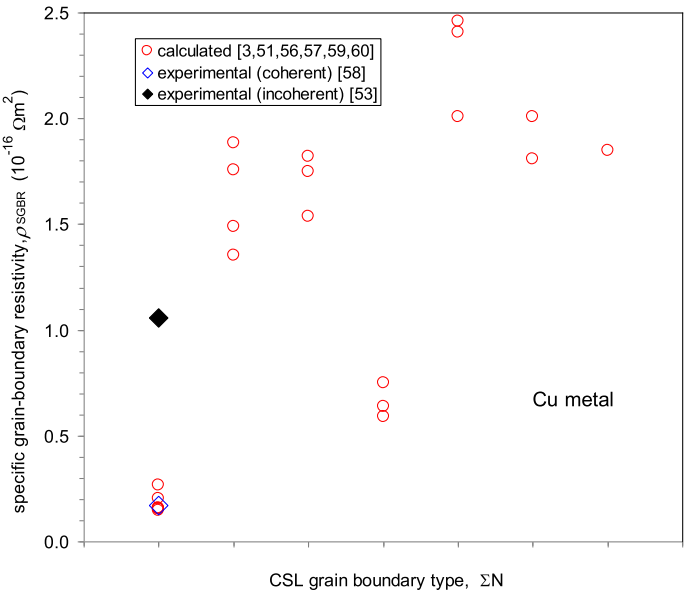

Fig. 9 Results of theoretical calculations of ρ_{SGBR} for various CSL boundary types for Cu metal from reports as indicated in the legend. Experimental results for coherent (◇ [58]) and incoherent (◆ [53]) Σ3 boundaries are also included

parameters are to be derived as noted already in Sect. 2.2.1 in connection with the results of Chawla et al. [44].

4.3 Grain-boundary reflection coefficient R for Ni and Cu: experiment vs. theory

As far as the grain-boundary reflection coefficient R is concerned, we have summarized the relevant experimental data in Table 1. According to this, the value of R(Ni) can be expected to be between 0.35 and 0.70, depending on what is the real value of the electron mean free path for Ni metal. This range of possible R values was derived in this paper from the experimental A(Ni) value as well as from the MS fit in this work to the reference $\rho_{exp}(d)$ data for Ni.

Based on the data in Table 1 and the discussion in Sect. 3.2.1, in our opinion the best experimental value of the grain-boundary reflection coefficient for Cu metal is R(Cu) = 0.46(3). This data and its error range comprises the R(Cu) values derived by various careful MS and MS + FS fits of Sun et al. [1] to their experimental resistivity vs. grain size data on Cu films and is also conform to the experimental resistivity vs. grain size data of Andrews et al. [35] on massive Cu specimens.

As to the theoretical assessment of R for metals, Zhu et al. [46] set up a model by assuming that R can be related to the bonding energy between the atoms of the given metal. As a measure of the bond strength, they took the melting temperature T_m. They started by considering that if R is the reflection coefficient, then 1-R is the tunneling probability of an electron with a kinetic energy smaller than the potential barrier represented by a grain boundary. Making the rather arbitrary assumption that the width of the potential barrier is 1/3 of the bond length and using average values of some thermodynamic parameters for metals, after numerous simplifications they arrived at a relation according to which R is a function of the melting temperature only: $R = 1 - 4/[\exp(T_m{}^{1/2}) + 2]$ where T_m is taken in kelvin units. By using

the standard melting temperatures [62] T_m(Cu) = 1358 K and T_m(Cu) = 1728 K, their formula yields R(Cu) = 0.372 and R(Ni) = 0.450. Although it is hard to conceive that such a simple treatment can really properly account for the grain-boundary resistivity, the derived R values are at least qualitatively compatible with the above derived experimental values of the reflection coefficients of Ni and Cu.

We are furthermore aware of a few more theoretical attempts [3, 61, 63] to derive R(Cu) for various CSL type grain boundaries on the basis of first-principles calculations of the electronic transport. Apart from the case of the twin boundary ($\Sigma 3$), the other R(Cu) data of these calculations [3, 61, 63] mainly fall in the range 0.1 to 0.2 which is at least by a factor of 2 below the average value R(Cu) = 0.46(3) we derived above from available experimental data on polycrystalline Cu specimens with random grain boundaries. The much lower grain-boundary reflection coefficient $R(\Sigma 3) = 0.0164$ [3] calculated for the coherent twin boundary complies well with the correspondingly low value of $\rho_{SGBR}(\Sigma 3)$ both from experiments and theory (cf. Fig. 9).

It may be illuminating to reveal a correlation between the calculated ρ_{SGBR}(Cu) and R(Cu) values of César et al. [3]. A correlation between the calculated values of the two parameters (open circles) is clearly seen in Fig. 10 where we can observe that the calculated data follow a linear variation of R with ρ_{SGBR} as indicated by the thin solid line getting well through the calculated values. Although not in a linear fashion, but a monotonous increase of R with increasing ρ_{SGBR} could already be anticipated via Eq. (15) by noting that $\rho_{SGBR} \propto A$ according to Eq. (5). Using Eq. (15) with the average value of the stereological proportionality factor $<k_{GB}> = 2.82$, we calculated the R values from the theoretical values of ρ_{SGBR} and these data are shown by the solid circles in Fig. 10. The extrapolation of these latter data indicated by the thick solid line goes smoothly towards the experimental data pair of R and ρ_{SGBR}. This might be interpreted in a manner that, by assuming that the theoretical ρ_{SGBR} values [3] correctly correspond to the specific grain-boundary resistivity of the increasingly more complex CSL type grain boundaries considered in the theoretical analysis, these ρ_{SGBR} values can be converted into R values approaching properly the grain-boundary reflection coefficient of Cu metal as derived in the present work for polycrystalline Cu specimens with random grain boundaries.

A further justification for this interpretation may be taken from the results of Dixit et al. [61] since by adding their calculated R(Cu) and ρ_{SGBR}(Cu) data pair to Fig. 10 (solid triangle), it fits well into the trend of the already displayed data.

It may still be worth mentioning the theoretical efforts of Rickman and Barmak [64] who examined the impact of microstructural features on the electrical conductivity of metallic thin film by using Monte Carlo simulations. They calculated the conductivity of a model structure with various numbers of cells (grains) as a function of the grain-boundary electron transmission coefficient. Their model result for R was in fairly good agreement with the corresponding experimental value of Sun et al. [1] derived from experiments on thin Cu films.

5 General comments on the two data evaluation approaches and on Matthiessen's rule

The basic feature of the approach of Andrews [15] was his experimental observation that besides the bulk resistivity ρ_{bulk} due to phonons and lattice defects, there is a resistivity contribution (ρ_{GB}) proportional to the amount of grain-boundary surface area per unit volume of the specimen. According to stereological considerations (see "Appendix A.1"), the latter quantity is inversely proportional to the average grain diameter. Therefore, the total resistivity

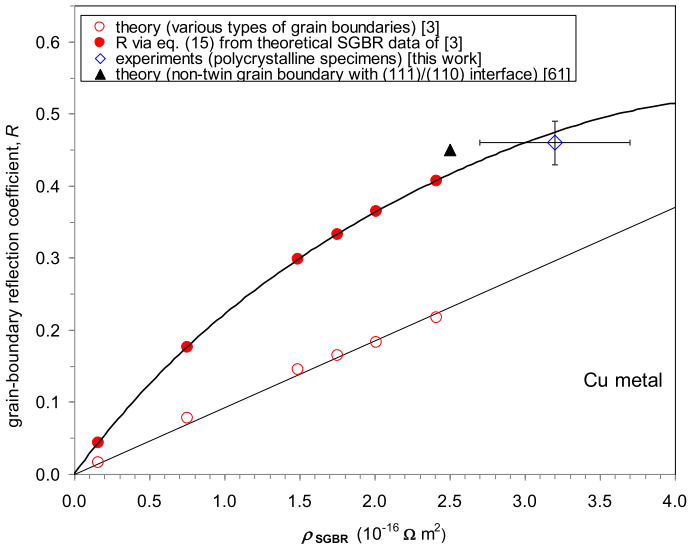

Fig. 10 Correlation between the grain-boundary reflection coefficient R and the specific grain-boundary resistivity ρ_{SGBR} from experiments and theory for Cu metal. The diamond symbol represents the best experimental value for the two parameters as derived in the present work for random grain boundaries in polycrystalline Cu specimens. The open circles are the calculated values for specific individual CSL grain boundaries of various types in Cu [3]. The thin solid line indicates a linear trend between the two theoretically derived parameters. The solid circles were obtained by us from the theoretically calculated ρ_{SGBR} values of Ref. [3] via Eq (15) by using $<k_{\mathrm{GB}}> = 2.82$. The thick solid line represents the trend of the solid circles and their extrapolation towards the experimental data pair. The solid triangle indicates the theoretically calculated data of Dixit et al. [61] for a non-twin grain boundary with (111)/(110) interface

of a specimen containing also grain boundaries can be written as $\rho = \rho_{\mathrm{bulk}} + \rho_{\mathrm{GB}} = \rho_{\mathrm{bulk}} + A/d$ [see Eqs. (1) and (6)]. This relation was shown to be valid in the present paper for both Ni and Cu under conditions when surface scattering due to the finite specimen dimensions can be neglected. It is important to emphasize for the approach of Andrews [15] that no model assumptions are necessary to quantitatively describe the grain-size dependence of the resistivity and to extract an experimental parameter (A) characterizing the grain-boundary resistivity.

The physical picture behind the Andrews approach [15] is that we can assign a definite resistivity value to the unit surface area of a grain boundary, the latter considered as a wall of finite thickness. As discussed above, delicate measurements [43, 51–53] have demonstrated that, indeed, there is a definite resistivity increment when measuring the resistivity of a thin strip specimen containing a single grain boundary in comparison with an identical strip without grain boundary.

As far as the Mayadas–Shatzkes model [14] is concerned, it relies on the introduction of a reflection coefficient R characterizing the reflecting capability of grain boundaries for conduction electrons. In this model, the grain boundaries are considered as planes characterized by a potential on which the electrons can be scattered and the scattering results either in a reflection or a transmission of the electron impinging on the potential wall. Thereby, a resistivity contribution arises which is proportional to the probability of the electron reflection characterized by the reflection coefficient R. Evidently, R is a monotonically increasing function of the grain-boundary scattering potential. In this manner, the reflection coefficient

R which contains information on the scattering potential of the grain boundaries should also appear in the resistivity term characterizing the grain-boundary contribution. The total resistivity formula in the MS model, $\rho_{MS}(d)$, indeed results in larger resistivity for larger R as is demonstrated in Figs. 2, 3, 4, 5, 6, 7, and 8.

We should also make some notes on the reliability of the two approaches used for evaluating the experimental data. As mentioned above, the phenomenological Andrews approach does not require any model assumptions and as long as the resistivity vs. grain size data can be described by the empirically found formula of Andrews [15], i.e., Eq. (6), the analysis yields a reliable experimental parameter for the grain-boundary contribution to the resistivity.

On the contrary, there is a basic problem with the MS model already from the starting point. Namely, Mayadas and Shatzkes [14], while attempting to solve the Boltzmann equation for electron transport, made the assumption that the scattering of electrons on grain boundaries can be characterized by a relaxation time, similarly to the background (bulk) scattering events and, thus, there is an effective relaxation time for the whole conduction process. This treatment is equivalent to the assumption of the validity of Matthiessen's rule. On the other hand, Landauer [65] pointed out already more than a decade before the work of Mayadas and Shatzkes [14] that if grain boundaries imagined as reflecting walls are also present, there is no single relaxation time for the whole conduction process which statement is just in opposition to the basic assumption of Mayadas and Shatzkes [14]. Particularly Vancea and coworkers [18, 19] gave strong arguments towards the inappropriateness of the MS model due to the Landauer-type deficiency. We have also raised already this issue [20] by noting that the reason for the fact that no relaxation time can be defined for the grain-boundary scattering event may be that this type of scattering process cannot be treated on equal footing with the stochastic processes such as scattering on point or line defects and phonons. This is because at the grain boundaries which are two-dimensional defects, an electron always undergoes a scattering when it impinges on the grain boundary after having travelled a distance equal to the average grain diameter if the latter is smaller than the electron mean free path.

We should refer at this point to the work of Munoz and Arenas [2] which provided a quantum approach to the theory of the transport properties in nanometric metallic structures, including also scattering at grain boundaries. These authors also formulated a strong criticism towards the foundations of the MS model and this criticism confirms the above described concerns about its reliability. An important issue in the work of Munoz and Arenas [2] is the question of the validity of Matthiessen's rule. They point out properly that the MS model [14] actually assumes the validity of Matthiessen's rule when an effective relaxation time is introduced. Furthermore, Munoz and Arenas [2] found that the quantum mechanical treatment of simultaneous bulk and grain-boundary scattering leads to a violation of Matthiessen's rule.

On the other hand, we have demonstrated in the present paper that the Andrews method properly describes the experimental grain-size dependence of the resistivity in the form $\rho = \rho_{bulk} + \rho_{GB} = \rho_{bulk} + A/d$ which formally looks as if Matthiessen's rule were valid for the resistivity of a metal in which not only bulk scattering events occur, but also scattering on grain boundaries. A key point is, however, that the Andrews method does not rely on the relaxation time approximation and on the electron mean free path concept, but rather simply formulates the empirically observed fact about the additivity of two resistivity contributions in accounting for the resistivity in the presence of grain boundaries. So the agreement with a Matthiessen's rule type behavior of the Andrews approach [15] is only formal since the description in the Andrews method does not consider the electron scattering event at grain boundaries as a stochastic process in contrast to the MS model [14] relying on the relaxation time approximation.

The above discussed controversial issue is certainly strongly connected with another concern related to the electron mean free path λ. For a metal with a given average grain size, when reducing the temperature T, one would expect a signature in the evolution of the $\rho\ (T)$ curve somewhere at the temperature where λ becomes smaller than the average grain size, whereas experimentally there is no such signature around this critical temperature. Similarly, when at constant temperature we vary the grain size d, one cannot see again any irregularity of the $\rho\ (d)$ curve around the grain size where d becomes comparable with or equal to λ. A theory describing the resistivity as a function of grain size or temperature should account also for the lack of such signatures in the $\rho\ (d)$ or $\rho\ (T)$ curves around the critical grain size or temperature, respectively.

Another related evident controversy arises also from the reflection coefficient data of Table 1. Namely, when using the experimentally derived electron mean free path values for Ni and Cu, we arrived at R(Ni) ~ 0.35 and R(Cu) ~ 0.46. It follows from these data that R(Ni) < R(Cu) what strongly contradicts to expectation about the relation between the grain-boundary reflection coefficients of these two metals by considering that at finite temperatures, the resistivity of Ni is much larger than that of Cu and, also, A(Ni) ~ 2 A(Cu).

It is clear from the foregoing discussion that although a lot of issues have already been clarified concerning the electron transport processes in nanometric and nanocrystalline metallic structures, there are still some controversies which require further efforts to understand their origin.

6 Summary

In the present paper, reported literature data on the grain-size dependence of resistivity of Ni and Cu metals were critically evaluated. In this evaluation, the results of those reports were only considered where direct imaging by various microscopy methods was used to determine the grain size (reports with XRD-based structural characterization only are discussed separately in "Appendix B"). By this careful data analysis, we have selected those $\rho_{exp}(d)$ data sets which can be considered as reference data characterizing the grain-size evolution of resistivity in polycrystalline Ni and Cu metals with random grain boundaries. From these, we have then derived the current best room-temperature values of the Andrews parameter A, the specific grain-boundary resistivity ρ_{SGBR} and the reflection coefficient R for Ni and Cu metals which are summarized in Table 1. Since the $\rho_{exp}(d)$ data were obtained on polycrystalline specimens, the deduced parameters represent average values over all possible grain boundary types and orientations.

Particular attention was paid to analyzing each reported data set, for the first time, by using both customarily applied approaches, namely the Andrews method [15] and the Mayadas–Shatzkes model [14] which represent conceptually different approaches in accounting for the contribution of grain boundaries to the total resistivity as discussed in Sect. 5.

The experimental data were also confronted with theoretical calculations of the specific grain-boundary resistivity and the reflection coefficient of various types of grain boundaries and, apart from the twin-boundary resistivity, there is still room for improving the theoretical calculations for achieving a better matching with experiments.

An important suggestion from our analysis is that due to the uncertainties of the data extraction in the MS model, for the evaluation of the experimental resistivity data in metallic specimens with various grain sizes, the Andrews method should always be tested first. Namely, if this method describes well the grain-size dependence of the resistivity, then we can derive a reliable experimental parameter characterizing the resistivity contribution of

grain boundaries for that particular metal. This parameter can then be safely compared with similar results for other metals or with results of theoretical calculations.

As to the MS model, it is emphasized again that although we are aware of the deficiencies of its foundations as discussed both in the Introduction and in Sect. 5, we still used it in data evaluation for completeness since many literature results were reported in this framework. A comparison with the Andrews approach revealed that there is often a good correspondence between the parameters of the two data evaluation approaches in spite of the apparent deficiencies of the classical MS model.

It is hoped that the outlined considerations will instigate further experimental and theoretical efforts to clarify the microscopic features of the transport processes in the presence of grain boundaries.

Acknowledgements The Wigner Research Centre for Physics utilizes the research infrastructure of the Hungarian Academy of Sciences and is operated by the Eötvös Loránd Research Network (ELKH) Secretariat, Hungary. The first considerations on comparing the Andrews method and the MS model were elaborated during a short-term scientific mission of the author to the Strathclyde University, Glasgow, which was supported by the COST Action MP1407; the kind hospitality of S. Roy in Glasgow is gratefully acknowledged. Comments by L. Péter provided useful help for improving the manuscript. The author is indebted to J. Gubicza for discussions on structural analysis by XRD. Special thanks are expressed to the two reviewers for their constructive criticism towards better articulating the main message of the paper.

Data Availability Statement The data that support the findings of this study are available from the author upon reasonable request.

Funding Open access funding provided by ELKH Wigner Research Centre for Physics.

Appendix

A. Frameworks for evaluating grain-boundary resistivity contributions in metals from experimental data

A.1 Andrews method

The first attempt to account for the grain-boundary resistivity contribution was the work of Andrews [15] who noticed that, while studying the resistivity of massive Cu metal samples with various grain sizes in the micrometer range, there was a resistivity contribution proportional to the grain-boundary surface area (S_{GB}) per unit volume, i.e., to S_{GB}/V.

The total resistivity ρ_A in the Andrews approach is written as

$$\rho_A = \rho_{bulk} + \rho_{GB} \tag{1}$$

where ρ_{bulk} is the resistivity of the defect-free and impurity-free state with large grains (this will be referred to as the bulk state) and ρ_{GB} is the total grain-boundary contribution to the resistivity. The grain boundaries were considered as walls which are characterized by a

certain resistivity contribution per unit grain-boundary area. Accordingly, ρ_{GB} is proportional to S_{GB}/V and, thus, we can write

$$\rho_{GB} = \rho_{SGBR} S_{GB}/V \tag{2}$$

which expression is used to define the specific grain-boundary resistivity ρ_{SGBR}, i.e., the resistivity increment due to the grain-boundary surface area per unit volume.

According to stereological considerations [66, 67], S_{GB}/V is generally considered to be inversely proportional to the average grain diameter d, i.e.,

$$S_{GB}/V = k_{GB}(1/d) \tag{3}$$

with the constant proportionality factor k_{GB}. Then, the total grain-boundary resistivity is

$$\rho_{GB} = \rho_{SGBR}\, k_{GB}/d = A/d \tag{4}$$

where we have introduced the Andrews parameter

$$A = k_{GB}\rho_{SGBR} \tag{5}$$

Accordingly, in the Andrews approach, we have for the total resistivity

$$\rho_A = \rho_{bulk} + A/d \tag{6}$$

As demonstrated in Sect. 2 on the basis of numerous reports on Ni and Cu, the grain-size dependence of the resistivity can be well described by Eq. (6) and in such cases, the Andrews parameter A is an experimentally well-defined quantity.

There have been various approaches to determine the proportionality factor k_{GB} relating the quantity S_{GB}/V with the mean grain diameter d, which relation is an important topic in the field of stereology, but a few of them are only mentioned here. According to Smith and Guttman [66], for a random three-dimensional structure of contiguous grains, the grain-boundary surface area per unit volume can be expressed as $S_{GB}/V = 2/c$ where c is the mean linear intercept distance or mean chord length which is the average distance between the intercepts of a randomly directed line with successive grain boundaries as often applied when evaluating grain-size images. Furthermore, for a wide range of size distributions of nearly equi-axed (i.e., not severely elongated) grains, Hensler [67] found that the conversion from the mean chord length c to the mean grain diameter d is given by the expression $d = 16\, c/\pi^2 \approx 1.62\, c$. Combining the two above expressions, we finally arrive at the relation $S_{GB}/V = 32/(\pi^2\, d) \approx 3.24/d$., i.e., $k_{GB} = 3.24$ in this case. In contrast to this general treatment for any general grain shape, Table 4–1 of the book of DeHoff and Rhines [68] gives S_{GB}/V values for specific regular, equal-sized and space-filling grain shapes (cube, hexagonal prism, rhombic dodecahedron and truncated octahedron) not in terms of the overall grain diameter, but rather expressed with a linear dimension on one of the flat faces of the polyhedron. Later some authors [69, 70] used $k_{GB} = 2.37$ in Eq. (3), whereas others [15, 35] used $k_{GB} = 2.7$ when converting their experimental data into ρ_{SGBR}. Due to these differences in the k_{GB} factors applied in various studies when relating S_{GB}/V and d, evidently, care should be exercised when comparing results of different studies on a given metal or results on different metals to reveal what was the actual value of k_{GB} when converting between A and ρ_{SGBR}. Therefore, it is emphasized again that our suggestion is to use primarily the Andrews parameter A when discussing experimental data for the grain-boundary resistivity since in this case the stereological problem of converting the measured average grain diameter into surface area per unit volume (i.e., the exact value of the proportionality factor k_{GB}) does not interfere with the evaluation of experimental data.

A.2 Mayadas–Shatzkes (MS) model

While studying the resistivity of Al thin films, Mayadas [71] realized that the thickness dependence cannot be described by the Fuchs–Sondheimer (FS) model [6, 7] with a constant intrinsic (bulk) resistivity. It was necessary to assume a thickness-dependent intrinsic resistivity which was ascribed to the presence of grain boundaries due to the small grain size in the film. This conclusion prompted Mayadas and coworkers [14, 72] to elaborate a model for thin film resistivity in order to account not only for the scattering of electrons at external surfaces (FS model), but also at internal surfaces (such as grain boundaries). The basic features of the MS model can be summarized as follows.

The thin film is considered as consisting of columnar grains extending from the bottom to the top of the film. Those grain boundaries are taken only as effective scatterers the plane of which is perpendicular to the electron flow direction and they are characterized with a short-ranged scattering potential of given height (δ-function potential). The positions of the two-dimensional grain-boundary planes are randomly distributed along the electron pathway with an average separation d corresponding to the mean column diameter (or grain size) and between the grain-boundary positions an isotropic background scattering caused by point defects and phonons is assumed, corresponding to the scattering in the bulk state of the film material.

After formulating the Boltzmann equation in the relaxation time approximation for the above outlined model of the resistivity of a thin film, Mayadas and coworkers [14, 72] found a solution under the condition that there is a single effective relaxation time τ^* for the simultaneous background (bulk) scattering and grain-boundary scattering and τ^* is given by

$$1/\tau^* = 1/\tau_{\text{bulk}} + 1/\tau_{\text{GB}} \tag{7}$$

where τ_{bulk} and τ_{GB} are the relaxation times for the background and grain-boundary scattering, respectively.

Along this line, the total resistivity $\rho_{\text{MS}}(d)$ in the MS model could finally be written as

$$\rho_{\text{MS}}(d) = \rho_{\text{bulk}} f(\alpha) \tag{8}$$

where the function $f(\alpha)$ is defined as

$$f(\alpha) = [1 - (3/2)\alpha + 3\alpha^2 - 3\alpha^3 \ln(1 + 1/\alpha)] - 1 \tag{9}$$

with

$$\alpha = (\lambda_{\text{bulk}}/d)R/(1 - R). \tag{10}$$

In the last expression, λ_{bulk} is the electron mean free path in the bulk state at the temperature of the experiment and R is the electron reflection coefficient from a grain-boundary wall characterized by the chosen scattering potential (by definition, we have the relation $0 < R < 1$). Accordingly, the MS model treats the grain boundaries as potential walls on which the impinging electrons are scattered and, upon scattering, the probability of reflection is R, whereas the transmission probability is $1 - R$. Since the total resistivity in the presence of grain boundaries is larger than the bulk value ($\rho_{\text{MS}} > \rho_{\text{bulk}}$), it follows that $f(\alpha) > 1$. We can also see that according to Eq. (8), the total resistivity in the presence of grain boundaries is proportional to the bulk resistivity in the MS model.

It should be noted that Eq. (8) describes the thin film resistivity only in the case when surface scattering by the FS model can be neglected, e.g., for sufficiently thick films. Of course, the effects of surface scattering and grain-boundary scattering can also be combined

as formulated already by Mayadas and Shatzkes [14], but in the present paper we restricted discussion to experimental studies only in which the surface scattering can be neglected in comparison with the background and grain-boundary scattering, i.e., for massive specimens and not too thin films.

The derivation of the reflection coefficient R from experimental data proceeds in a manner that one first calculates the $\rho_{MS}(d)$ resistivity as a function of grain size d for various R values with constant λ_{bulk} corresponding to the mean free path of the metal under study at the measurement temperature. Then, these calculated $\rho_{MS}(d)$ functions are compared to the experimentally measured $\rho_{exp}(d)$ curves to find the R value for which $\rho_{MS}(d)$ agrees with $\rho_{exp}(d)$. This evaluation can be performed either for massive materials or for thin films with negligible surface scattering, the latter condition strongly varying with temperature due to the strong increase of the electron mean free path with decreasing temperature in pure metals.

A.3 Relation between parameters A and R

It was pointed out by Mayadas and Shatzkes [14] that in the limit of $\alpha << 1$, their function f(α) as given in Eq. (9) simplifies to [1 + (3/2)α]. Therefore, in this limit, Eq. (8) can be written as

$$\rho_{MS}(d) = \rho_{bulk}[1 + (3/2)\alpha]. \tag{11}$$

Expanding this expression and substituting α from Eq. (10), we end up with

$$\rho_{MS}(d) = \rho_{bulk} + (3/2)(\rho_{bulk}\lambda_{bulk}/d)R/(1 - R). \tag{12}$$

It is easy to recognize that Eq. (12) corresponds to Eq. (1) of the Andrews method if we identify the second term of Eq. (12) with the total grain-boundary contribution to the resistivity:

$$\rho_{GB} = (3/2)(\rho_{bulk}\lambda_{bulk}/d)R/(1 - R). \tag{13}$$

Furthermore, from Eq. (13) we can deduce, by comparison with Eq. (4), that the Andrews parameter can be expressed with the help of R as follows:

$$A = (3/2)\rho_{bulk}\lambda_{bulk}R/(1 - R). \tag{14}$$

We can also reverse this expression and then get

$$R = [1 + (3/2)\rho_{bulk}\lambda_{bulk}/A]^{-1}. \tag{15}$$

We have applied Eq. (15) to calculate the R(Ni) and R(Cu) values by using the corresponding A values determined from an Andrews fit to the experimental data for Ni and Cu. As can be seen in Table 1, we obtained in this manner R values which are only slightly smaller than the corresponding values of R obtained from a direct $\rho_{MS}(d)$ fit to the experimental $\rho_{exp}(d)$ data for both metals. This demonstrates that once we have reliable experimental resistivity vs. grain size data sets for a given metal, and the data can be fitted by the Andrews method (i.e., the resistivity contribution due to grain boundaries scales with the inverse of the grain size), we can then derive the grain-boundary reflection coefficient with Eq. (15) provided, furthermore, that we also know the electron mean free path at the measurement temperature. If there is any uncertainty in the mean free path value, the Andrews parameter still correctly characterizes the grain-boundary resistivity contribution for the given metal without any model assumption. It should also be noted that the validity of the application of Eq. (15), i.e., to convert the A value to an R value, depends on the fulfillment of the condition $\alpha =$

$(\lambda_{bulk}/d)R/(1-R)<<1$. In the last column of Table 1, we have determined the fulfillment of this condition for those R values which were derived from Eq. (15). The data in the last column indicate that this condition is fulfilled only if $d>135$ nm for Ni and if $d>335$ nm for Cu. In spite of this restriction, the A values derived from experimental resistivity data either below or above the limit for Cu and mainly below the limit for Ni can be fairly well converted to practically the same R value as obtained from a direct MS fit (i.e., by applying Eq. 8) to the experimental data. This implies that the validity of Eq. (15) may extend also beyond the fulfillment of the condition $\alpha<<1$.

On the other hand, particular care should be exercised when converting the parameters of the Andrews method and the MS model as we can see on the example of the erroneous derivation of the grain-boundary reflection coefficient of Cu by Mayadas and Shatzkes [14] from the experimental data of Andrews et al. [35]. Mayadas and Shatzkes [14] used the correct value $[\rho_{bulk}\lambda_{bulk}]_{Cu}=6.6\times10^{-16}$ Ωm^2, but mistakenly put $\rho_{SGBR}(Cu;4.2\ K)=3.12\times10^{-16}$ Ωm^2 [35] equal with the right hand side of Eq. (14), i.e., they replaced in this equation the Andrews parameter $A(Cu;4.2\ K)=8.42\times10^{-16}$ Ωm^2 [35] with $\rho_{SGBR}(Cu;4.2\ K)$ which quantities differ by the factor $k_{GB}=2.7$ [35] and so Mayadas and Shatzkes arrived at $R(Cu;4.2\ K)=0.24$. If we calculate R correctly, i.e., we put in Eq. (14) the value $A(Cu;4.2\ K)=8.42\times10^{-16}$ Ωm^2 [35], then we get $R(Cu;4.2\ K)=0.460$. A comparison of the above correctly deduced $R(Cu;4.2\ K)=0.460$ value with the $R(Cu,300\ K)$ values in Table 1 reveals a good agreement. Furthermore, Mayadas and Shatzkes [14] made the same error when calculating $R(Al;4.2\ K)=0.17$ (with the help of $[\rho_{bulk}\lambda_{bulk}]_{Al}=8.2\times10^{-16}$ Ωm^2) since by using the experimental value $A(Al;4.2\ K)=6.61\times10^{-16}$ Ωm^2 [35] instead of $\rho_{SGBR}(Al;4.2\ K)=2.45\times10^{-16}$ Ωm^2 [35], we get the correct value as $R(Al;4.2\ K)=0.350$. It should be noted that by using the recent theoretical value $[\rho_{bulk}\lambda_{bulk}]_{Al}=5.01\times10^{-16}$ Ωm^2 [5] and the experimental value $A(Al;4.2\ K)=6.61\times10^{-16}$ Ωm^2 [35], we get $R(Al;4.2\ K)=0.468$.

B. Comparison of structural parameters deduced from XRD line broadening and direct microstructure imaging

It has been pointed out in our previous work [16] that from the viewpoint of electrical transport the average grain size d as deduced from direct imaging by various microscopy methods (optical microscopy, TEM, EBSD or FIB imaging) is the relevant structural parameter and not the mean crystallite size x which can be derived by various methods from the broadening of XRD lines [16, 73–77]. This is because the grains directly imaged and measured by TEM contain also coherency-breaking intragrain defects such as, e.g., small-angle grain boundaries, twin boundaries and stacking faults. In addition to the XRD line broadening due to the small grain size (i.e., due to the finite size of the coherently scattering domains [73]), the intragrain defects also contribute to the XRD line broadening and, thus, have an effect on the mean crystallite size x. On the other hand, these defects have a much smaller specific resistivity than the grain boundaries as evidenced both experimentally [35, 43, 58, 78–80] and theoretically [3].

Furthermore, for film or foil samples which are typically used for measuring the resistivity, the commonly applied XRD techniques performed in reflection mode provide the crystallite size x only in the direction perpendicular to the film/foil plane. On the other hand, from the viewpoint of electron scattering, the grain boundaries perpendicular to the film/foil plane are the really important features since the measuring current flows in the plane and the average distance between these latter grain boundaries, i.e., lateral grain size, cannot be revealed by these conventional XRD methods. Therefore, in the core part of the present paper, we have

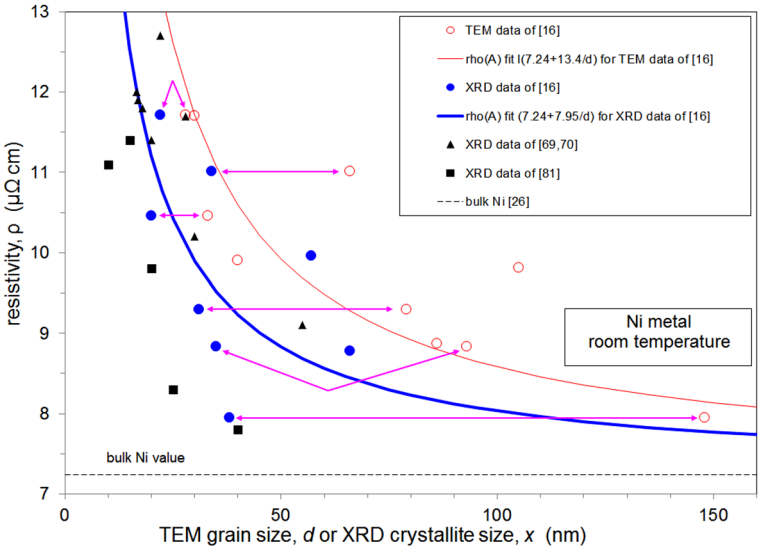

Fig. 11 Resistivity ρ at room temperature as a function of the TEM grain size d (open circles) and/or the XRD crystallite size x (full circles) for electrodeposited nc-Ni from our previous work [16]. Arrows connecting an open and a full circle indicate that the XRD and TEM study was carried out on the same sample. The thin solid line represents a fit according to the Andrews method to Eq. (6) with fixed $\rho_{\text{bulk}} = 7.24$ μΩ cm [26] and with fitted value $A_{\text{TEM}} = 13.4 \times 10^{-16}$ Ωm^2 for the data points displayed as a function of the TEM grain size and the thick solid line is the same with $A_{\text{XRD}} = 7.95 \times 10^{-16}$ Ωm^2 for the data points displayed as a function of the XRD crystallite size. The full triangles [69, 70] and squares [81] are also XRD-based data on electrodeposited nc-Ni

evaluated the data of only those resistivity reports where the lateral grain size was determined by direct microscopy imaging.

Before discussing here those reports where XRD was only used for structural characterization, first we demonstrate what is the consequence of displaying resistivity data as a function of the mean crystallite size x on the evaluation of the grain-boundary resistivity contribution as often has been made in the past. At this point, we should note that the mean crystallite size is usually smaller than the average grain size ($x < d$) [16, 74–77] due to the additional broadening caused by the intragrain defects. To illustrate this, Fig. 11 displays the room-temperature resistivity data from our previous study [16] on electrodeposited nc-Ni as a function of the grain size d (open circles) derived from TEM imaging and/or the crystallite size x (full circles) derived from XRD patterns recorded with high accuracy in a wide angular range which were evaluated with the help of the extended Convolutional Multiple Whole Profile (eCMWP) fitting method [75–77]. For most of the samples, both XRD and TEM studies were carried out and these data pairs are connected by arrows in the plot, in addition to the results on a few samples with one kind of structural investigation only. It can be seen that the mean crystallite size x is systematically smaller than the grain size d for the same samples and also the other samples exhibit the same trend.

If we carry out now an Andrews fit according to Eq. (6) separately for the XRD-based and TEM-based data, we obtain the thin solid (TEM) and thick solid (XRD) fit lines with Andrews parameter values as $A_{\text{TEM}}(\text{Ni}) = 13.4 \times 10^{-16}$ Ωm^2 and $A_{\text{XRD}}(\text{Ni}) = 7.95 \times 10^{-16}$ Ωm^2. Evidently, the XRD-based resistivity data for the same samples not only appear as

shifted to the left, but their A(Ni) value deduced from the Andrews fit is also smaller by nearly a factor of 2 than the value obtained for the TEM-based data.

McCrea and coworkers [69, 70] also applied the Andrews method for analyzing their resistivity data on electrodeposited nc-Ni with crystallite sizes ranging from 17 to 55 nm which were determined by the Scherrer method [73] from the broadening of the main XRD line and their results are displayed by the full triangles in Fig. 11. By fitting their data to Eq. (6) and using $k_{GB} = 2.37$, McCrea and coworkers [69, 70] reported $\rho_{SGBR}(\text{Ni};295\ \text{K}) = 2.74 \times 10^{-16}\ \Omega\text{m}^2$ from which we can deduce $A_{XRD}(\text{Ni};295\ \text{K}) = 6.49 \times 10^{-16}\ \Omega\text{m}^2$. Madduri and Kaul [81] studied the resistivity of PP nc-Ni electrodeposits which were structurally characterized by recording XRD patterns evaluated by the Halder–Wagner method [82] to deduce the crystallite size and their results are represented by the full squares in Fig. 11.

According to Fig. 11, the XRD-based data by McCrea and coworkers [69, 70] and Madduri and Kaul [81] fall rather close to our XRD-based data (full circles) [16]. The differences between various reports [16, 69, 70, 81] are due to the fact that the various XRD evaluation methods applied in all these works lead, as discussed in Ref. [16], to a different crystallite size due to the different weighting procedures.

Nevertheless, Fig. 11 clearly demonstrates that evaluating the resistivity on the basis of the crystallite sizes derived from XRD leads to an underestimated value of the grain-boundary contribution to the resistivity with respect to an evaluation of the resistivity data on the very same specimens on a correct basis by using the directly imaged grain sizes.

Even if the absolute value of A(Ni) is incorrect when evaluated on the basis of the crystallite size, by using the low-temperature resistivity data reported in Refs. [69], [70] and [81], we have estimated from these data that the observed increase of A(Ni) from the liquid He range to room temperature is about 29% [69, 70] and 26% [81]. These results are somewhat larger than the other findings discussed in Sect. 2.1.1 for Ni and in Sect. 2.2.1 for Cu, but we should keep in mind that A(Ni) values deduced from the XRD-based data of Refs. [69, 70, 81] have certainly larger errors due to the lower number and larger scatter of these data (see Fig. 11) in comparison with the TEM-based data (see Figs. 1 and 4).

In the following, we discuss briefly the report of Wissmann [83] on evaporated Ni films for which the microstructure was studied by XRD to deduce the crystallite size x and the data were displayed as $\rho{\cdot}x$ vs. x which yielded a fairly linear plot. Fitting a straight line to these data, Wissmann [83] determined parameters which we converted into data corresponding to Eq. (6): $\rho_{bulk} = 12\ \mu\Omega\ \text{cm} + A/x$ with $A_{XRD}(\text{Ni};300\ \text{K}) = 28.8 \times 10^{-16}\ \Omega\text{m}^2$. In Fig. 12, the solid squares represent the resistivity variation of the Ni films of Wissmann [83] with these parameters in the investigated crystallite size range and the corresponding Andrews method fit to these data is displayed by the thick dashed line. The A value derived from the experimental data of Wissmann [83] is definitely too large by a factor of 2 with respect to the reference value on the basis of the TEM grain sizes [$A_{TEM}(\text{Ni};300\ \text{K}) = 14.7 \times 10^{-16}\ \Omega\text{m}^2$]. The reason for the much higher value of *A(Ni)* for the samples of Wissmann [83] comes partly from the fact that the bulk Ni resistivity value of $\rho_{bulk} = 12\ \mu\Omega$ cm deduced from the results on his samples is also well above the bulk Ni value of $\rho_{bulk} = 7.24\ \mu\Omega$ cm [26]. This is further underlined by the fact that, e.g., Reale [84] reported a resistivity value for a 10-nm-thick evaporated Ni film that was about half of the value obtained by Wissmann [83] for the same thickness. It is not clear what is the origin of the too high resistivities of the Ni films of Wissmann [83], but an increased surface roughness or an incidental contamination/oxidation of the films may have easily resulted in the excess resistivity observed. We mention this clearly overestimated A(Ni) result of Ref. [83] with emphasis since it was often cited in previous works as an experimental basis for comparison with theoretical calculations on Ni.

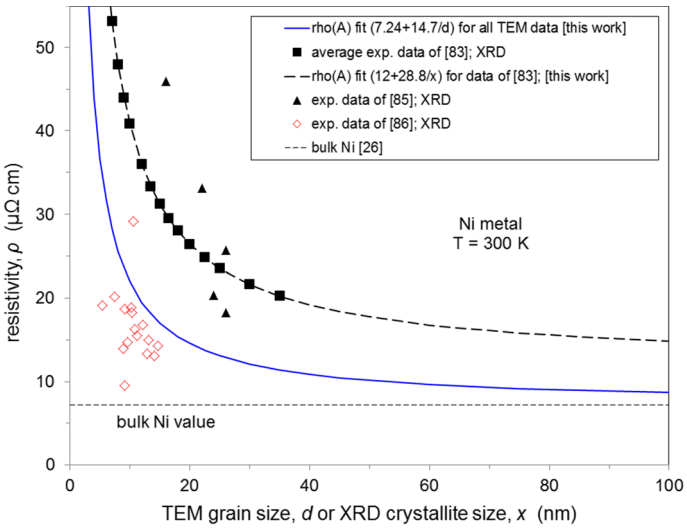

Fig. 12 Resistivity ρ at room temperature for Ni as a function of the TEM grain size d or the XRD crystallite size x. The solid line represents the fit according to the Andrews method to Eq. (6) with fixed $\rho_{\text{bulk}} = 7.24$ $\mu\Omega$ cm and with fitted value $A_{\text{TEM}} = 14.7 \times 10^{-16}$ Ωm^2 for the TEM-based data as obtained in this work (see Fig. 1). The solid squares represent the average XRD-based data on Ni thin films of Ref. [83] in the investigated crystallite size range. The dashed thick line corresponding to $\rho_{\text{bulk}} = 12$ $\mu\Omega$ cm and $A_{\text{XRD}} = 28.8 \times 10^{-16}$ Ωm^2 represents the fit according to Eq. (6) for the XRD-based data on Ni thin films of Ref. [83]. The solid triangle symbols and the open diamond symbols represent the XRD-based data of Ref. [85] and Ref. [86], respectively, on Ni thin films

The solid triangle symbols and the open diamond symbols in Fig. 12. are the data from Ref. [85] and [86] on evaporated Ni thin films, respectively, for which the microstructural characterization was performed by XRD. The resistivity data of Ref. [85] are close to the data of Wissmann [83] and are again evidently too large with respect to the TEM-based reference $\rho_{\text{exp}}(d)$ data (thick solid line in Fig. 12). On the other hand, we can see that the data of Ref. [86] are mostly close to the XRD-based data on Ni in Fig. 11 although some data points of Ref. [86] strongly deviate from the common trend (e.g., at about $x = 10$ nm, there are resistivity data with both 10 and 30 $\mu\Omega$·cm). This fact and, furthermore, the large difference in the resistivity values of Refs. [85] and [86], although reported from the same laboratory, underlines that in the case of thin films, sample preparation details influencing deposit quality may strongly influence the actual measured resistivities and, thus, also the deduced grain-boundary resistivity parameters.

We make a note also on the resistivity results of Mannan and Karim [87] on 100-nm-thick evaporated Cu films. These authors determined the XRD crystallite size x by the Scherrer method [72]. If we put their room-temperature resistivity values in Fig. 13 (solid circles), we can see that they fall well below the TEM-based reference data, a situation similar to what we could already see in Fig. 11 for Ni. Therefore, the grain-boundary resistivity data underestimated from the experimental results of Mannan and Karim [87], although also often referred to in the literature, once more underline the importance of the difference in the microstructure evaluation when performed by TEM and XRD.

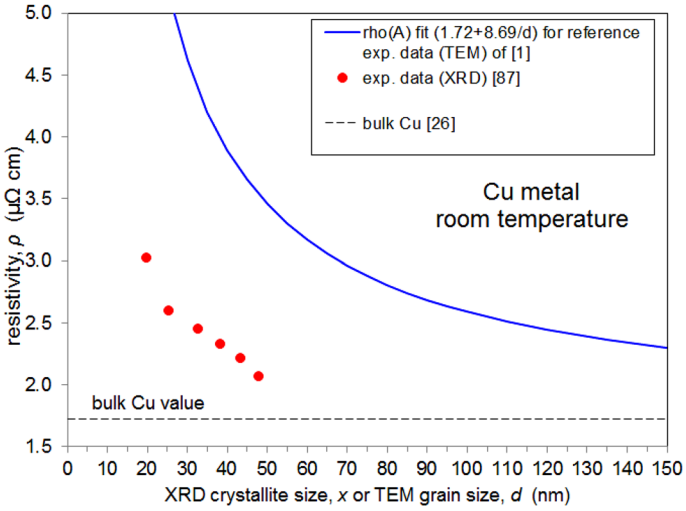

Fig. 13 Room-temperature resistivity ρ for Cu films as a function of the TEM grain size d or XRD crystallite size x as indicated in the legend. The solid line represents a fit to Eq. (6) with fixed $\rho_{\text{bulk}} = 1.72\ \mu\Omega$ cm [26] and with fitted value $A = 8.69 \times 10^{-16}\ \Omega\text{m}^2$ for the TEM-based data of Ref. [1] as obtained in this work. The solid circles represent the XRD-based data of Ref. [87]

C. Estimating the maximum resistivity of nc-Ni and nc-Cu

According to Eq. (6), the resistivity of a nc metal can be extremely large for very small grain sizes, but this is certainly unphysical. Therefore, in Ref. [16], we estimated the maximum possible resistivity for nc-Ni and this is briefly recalled here. By extrapolating the reported temperature dependence of the resistivity of liquid Ni metal to room-temperature, it was established [16] that the resistivity of the hypothetical amorphous Ni metal would be about 70 $\mu\Omega$ cm (uncertainty: $\pm 10\ \mu\Omega$ cm). This means that a massive Ni specimen at room temperature cannot have a resistivity larger than this value of the structurally most disordered (amorphous) state of Ni. Evidently, any crystalline state of Ni must also not exceed this limit at room temperature. Taking our best $A(\text{Ni};300\ \text{K}) = 14.7 \times 10^{-16}\ \Omega\text{m}^2$ value as determined in the present paper, with the help of Eq. (6) we can estimate that the room-temperature resistivity of nc-Ni reaches 70 $\mu\Omega$cm at a grain size of about $d = 2.3$ nm (due to the above specified uncertainty of the room-temperature resistivity of amorphous Ni, the corresponding possible d range is from 2 nm to 2.8 nm). Based on the known models for the grain-boundary and intercrystalline volume fraction [88] and taking 1 nm for the grain boundary thickness, we could then deduce [16] that at a grain size of $d = 2.3$ nm, the fraction of atoms within the crystallites reduces to about 20%, whereas the fraction of atoms in both the grain boundaries and in the triple-line junctions amounts to about 40%. This means that in nc-Ni at 2.3 nm grain size most of the atoms are in a topologically rather disordered state eventually very similar to an amorphous state so the material can indeed have a resistivity corresponding to that of amorphous Ni.

We will now make the same estimate for the maximum room-temperature resistivity of a massive Cu specimen with decreasing grain size. Similarly as we did above for Ni, we will rely on the measured temperature dependence of the resistivity of liquid Cu [89] which is then extrapolated to room temperature. It is obtained from this extrapolation that the room-

temperature resistivity of the hypothetical amorphous Cu metal would be about 12.2 μΩ cm. This means that a massive Cu specimen at room temperature cannot have a resistivity larger than this value of the structurally most disordered (amorphous) state of Cu. Taking our best $A(\mathrm{Cu};300\ \mathrm{K}) = 8.69 \times 10^{-16}\ \Omega\mathrm{m}^2$ value as deduced in the present paper, with the help of Eq. (6) we can estimate that the room-temperature resistivity of nc-Cu reaches 12.2 μΩcm at a grain size of about $d = 8.5$ nm. By assuming again a grain-boundary thickness of 1 nm and using the model of Palumbo et al. [88] on the grain-boundary and intercrystalline volume fraction, we can deduce that at a grain size of $d = 8.5$ nm, the fraction of atoms within the crystallites reduces to about 65%, and it is about 31% in the grain boundaries and about 4% in the triple-line junctions. This means that in nc-Cu at 8.5 nm grain size, about one third of the atoms are in a topologically rather disordered state and this seems to be sufficient to induce a resistivity increase making the total resistivity comparable to the resistivity of amorphous Cu. It follows from the above data that at $T = 300$ K, the resistivity of crystalline Cu increases upon complete structural disorder by a factor of 7.1 (= 12.2/1.72). This compares well to the corresponding resistivity increase of Ni at $T = 300$ K upon structural disorder by a factor of 9.7 (= 70/7.24).

By having a very similar relative resistivity increase of Cu and Ni upon structural disordering (with ratios 7.1 and 9.7, respectively), it is not a straightforward task to rationalize the different critical grain sizes of the two metals (Ni: 2.3 nm; Cu: 8.5 nm) at which the nc state reaches a resistivity equal to that of the amorphous (i.e., the structurally most disordered) state until we do not have a more detailed theoretical understanding of the influence of structural disorder on the electrical resistivity in Ni and Cu.

References

1. T. Sun, B. Yao, A.P. Warren, K. Barmak, M.F. Toney, R.E. Peale, K.R. Coffey, Surface and grain-boundary scattering in nanometric Cu films. Phys. Rev. B **81**, 155454 (2010)
2. R.C. Munoz, C. Arenas, Size effects and charge transport in metals: Quantum theory of the resistivity of nanometric metallic structures arising from electron scattering by grain boundaries and by rough surfaces. Appl. Phys. Rev. **4**, 011102 (2017). https://doi.org/10.1063/1.4974032
3. M. César, D.P. Liu, D. Gall, H. Guo, Calculated resistances of single grain boundaries in copper. Phys. Rev. Appl. **2**, 044007 (2014)
4. M. César, D. Gall, H. Guo, Reducing grain-boundary resistivity of copper nanowires by doping. Phys. Rev. Appl. **5**, 054018 (2016)
5. D. Gall, Electron mean free path in elemental metals. J. Appl. Phys. **119**, 085101 (2016)
6. K. Fuchs, The conductivity of thin metallic films according to the electron theory of metals. Math. Proc. Cambr. Philos. Soc. **34**, 100 (1938)
7. E.H. Sondheimer, The mean free path of electrons in metals. Adv. Phys. **1**, 1 (1952)
8. S.B. Soffer, Statistical model for the size effect in electrical conduction. J. Appl. Phys. **38**, 1710 (1967)
9. Y. Namba, Resistivity and temperature coefficient of thin metal films with rough surface. Jap. J. Appl. Phys. **9**, 1326 (1970)
10. J.R. Sambles, K.C. Elsom, The electrical resistivity of thin metal films with unlike surfaces. J. Phys. D **15**, 1459 (1982)
11. S.M. Rossnagel, T.S. Kuan, Alteration of Cu conductivity in the size effect regime. J. Vac. Sci. Technol. B **22**, 240 (2004)
12. J.M. Ziman, *Electrons and Phonons* (Clarendon Press, Oxford, 1960), Ch. VI.
13. A.F. Mayadas, R. Feder, R. Rosenberg, Resistivity and Structure of Evaporated Aluminum Films. J. Vac. Sci. Technol. **6**, 690 (1969)
14. A.F. Mayadas, M. Shatzkes, Electrical-resistivity model for polycrystalline films: the case of arbitrary reflection at external surfaces. Phys. Rev. B **1**, 1382 (1970)
15. P.V. Andrews, Resistivity due to grain boundaries in pure copper. Phys. Lett. **19**, 558 (1965)

16. I. Bakonyi, V.A. Isnaini, T. Kolonits, Zs. Czigány, J. Gubicza, L.K. Varga, E. Tóth-Kádár, L. Pogány, L. Péter and H. Ebert, The specific grain-boundary electrical resistivity of Ni. *Philos. Magaz.* **99**, 1139 (2019)
17. J.R. Sambles, The resistivity of thin metal films – some critical remarks. Thin Solid Films **106**, 321 (1983)
18. J. Vancea, G. Reiss, H. Hoffmann, Mean-free-path concept in polycrystalline metals. Phys. Rev. B **35**, 6435 (1987)
19. J. Vancea, Unconventional features of free electrons in polycrystalline metal films. Int. J. Mod. Phys. B **3**, 1455 (1989)
20. I. Bakonyi, E. Tóth-Kádár, J. Tóth, Á. Cziráki and B. Fogarassy, Electronic transport in nanocrystalline metals: a study of electrodeposited nickel foils. In: G.C. Hadjipanayis, R.W. Siegel (eds.): *Nanophase Materials.* NATO ASI Series E, Vol. 260, Kluwer Academic Publishers, Dordrecht, The Netherlands, p. 423 (1994)
21. M.J. Aus, B. Szpunar, U. Erb, A.M. El-Sherik, G. Palumbo, K.T. Aust, Electrical resistivity of bulk nanocrystalline nickel. J. Appl. Phys. **75**, 3632 (1994)
22. I. Bakonyi, E. Tóth-Kádár, L. Pogány, Á. Cziráki, I. Gerőcs, K. Varga-Josepovits, B. Arnold, K. Wetzig, Preparation and characterization of DC plated nano¬crystalline nickel electrodeposits. Surf. Coat. Technol. **78**, 124 (1996)
23. I. Bakonyi, B. Pula, E. Tóth-Kádár, I. Gerőcs, Á. Cziráki (unpublished); B. Pula, *M.Sc. Thesis* (Eötvös University, Budapest, Hungary, 1996).
24. E. Tóth-Kádár, I. Bakonyi, L. Pogány, Á. Cziráki, Microstructure and electrical transport properties of pulse plated nanocrystalline nickel electrodeposits. Surf. Coat. Technol. **88**, 57 (1997)
25. H.J. Cho, S. Wang, Y. Zhou, G. Palumbo, U. Erb, Thermal conductivity of bulk electrodeposited nanocrystalline nickel. Int. J. Heat Mass Transf. **100**, 490 (2016)
26. J. Bass, *Chapter 1: Electrical resistivity of pure metals and dilute alloys*. In: Landolt-Börnstein - Group III, New Series (Springer-Verlag, Berlin, Heidelberg, New York, 1982), Vol. 15a, pp. 1–287.
27. E.I. Tochitskii and N.M. Belyavski, Grain-boundary scattering effect on metal film resistivity. *phys. stat. sol. (a)* **61**, K21 (1980)
28. J.W.C. de Vries, Temperature-dependent resistivity measurements on polycrystalline SiO_2-covered thin nickel films. Thin Solid Films **150**, 209 (1987)
29. M.A. Angadi, Some transport properties of transition metal films. J. Mater. Sci. **20**, 761 (1985)
30. V. Starý, K. Šefčik, Electrical resistivity and structure of thin nickel films—effect of annealing. Vacuum **31**, 345 (1981)
31. N.W. Ashcroft and N.D. Mermin, *Solid State Physics* (Saunders College, Philadelphia, PA, USA, 1976 and Holt-Saunders Japan, Ltd., Tokyo, 1981)
32. E. Milosevic, P.Y. Zheng, D. Gall, Electron scattering at epitaxial Ni(001) surfaces. IEEE Trans. Electron. Dev. **66**, 4326 (2019)
33. D. Gall, The search for the most conductive metal for narrow interconnect lines. J. Appl. Phys. **127**, 050901 (2020). https://doi.org/10.1063/1.5133671
34. R.K. Islamgaliev, R.Y. Murtazin, L.A. Syutina, R.Z. Valiev, The role of grain boundaries in the electrical resistance of submicron grained nickel. Phys. Stat. Sol. **129**, 231 (1992)
35. P.V. Andrews, M.B. West, C.R. Robeson, The effect of grain boundaries on the electrical resistivity of polycrystalline copper and aluminium. Philos. Mag. **19**, 887 (1969)
36. M. Fenn, G. Akuetey, P.E. Donovan, Electrical resistivity of Cu and Nb thin films. J. Phys. Condense. Matter **10**, 1707 (1998)
37. N. Artunc, Z.Z. Öztürk, Influence of grain-boundary and surface scattering on the electrical resistivity of single-layered thin copper films. J. Phys. Condens. Matter **5**, 559 (1993)
38. P. Bruschi, C. Ciofi, V. Dattilo, A. Diligenti, A. Nannini, B. Neri, Copper metallizations for integrated circuits: TEM analysis and electrical characterization. J. Electr. Mater. **26**, L17 (1997)
39. S. Riedel, J. Röber, T. Gessner, Electrical properties of copper films produced by MOCVD. Microelectr. Eng. **33**, 165 (1997)
40. W. Wu, S.H. Brongersma, M. Van Hove, K. Maex, Influence of surface and grain-boundary scattering on the resistivity of copper in reduced dimensions. Appl. Phys. Lett. **84**, 2838 (2004)
41. P.K.F Woo, Thermal stability of nanocrystalline copper for potential use in printed wiring board applications (PhD Thesis, University of Toronto, 2011); unpublished, available at https://tspace.library.utoronto.ca/bitstream/1807/31975/3/Woo_Patrick_KF_201111_PhD_thesis.pdf
42. E.M. Dela Pena, S. Roy, Electrodeposited copper using direct and pulse currents from electrolytes containing low concentration of additives. Surf. Coat. Technol. **339**, 101 (2018)
43. I. Nakamichi, Electrical resistivity and grain boundaries in metals. Mater. Sci. Forum **207–209**, 47 (1996)
44. J.S. Chawla, F. Gstrein, K.P. O'Brien, J.S. Clarke, D. Gall, Electron scattering at surfaces and grain boundaries in Cu thin films and wires. Phys. Rev. B **84**, 235423 (2011)

45. R.S. Smith, E.T. Ryan, C.-K. Hu, K. Motoyama, N. Lanzillo, D. Metzler, L. Jiang, J. Demarest, R. Quon, L. Gignac, C. Breslin, A. Giannetta, S. Wright, An evaluation of Fuchs-Sondheimer and Mayadas-Shatzkes models below 14 nm node wide lines. AIP Adv. **9**, 025015 (2019)
46. Y.F. Zhu, X.Y. Lang, W.T. Zheng, Q. Jiang, Electron scattering and electrical conductance in polycrystalline metallic films and wires: impact of grain boundary scattering related to melting point. ACS Nano **4**, 3781 (2010)
47. R. Dimmich, Electronic transport properties of metallic multilayer films. J. Phys. F: Met. Phys. **15**, 2477 (1985)
48. N.F. Mott, The Electrical conductivity of transition metals. Proc. Roy. Soc. London A **153**, 699 (1936)
49. P.L. Rossiter, *The Electrical Resistivity of Metals and Alloys* (Cambridge University Press, Cambridge, 1987).
50. J.J. Bean, K.P. McKenna, Origin of differences in the excess volume of copper and nickel grain boundaries. Acta Mater. **110**, 246 (2016)
51. T.H. Kim, X.-G. Zhang, D.M. Nicholson, B.M. Evans, N.S. Kulkarni, B. Radhakrishnan, E.A. Kenik, A.P. Li, Large discrete resistance jump at grain boundary in copper nanowire. Nano Lett. **10**, 3096 (2010)
52. Y. Kitaoka, T. Tono, S. Yoshimoto, T. Hirahara, S. Hasegawa, T. Ohba, Direct detection of grain boundary scattering in damascene Cu wires by nanoscale four-point probe resistance measurements. Appl. Phys. Lett. **95**, 052110 (2009)
53. H. Bishara, M. Ghidelli, G. Dehm, Approaches to measure the resistivity of grain boundaries in metals with high sensitivity and spatial resolution: a case study employing Cu. ACS Appl. Electron. Mater. **2**, 2049 (2020)
54. R.A. Brown, Electrical resistivity of dislocations in metals. J. Phys. F **7**, 1283 (1977)
55. A.S. Karolik, A.A. Luhvich, Calculation of electrical resistivity produced by dislocations and grain boundaries in metals. J. Phys. Cond. Matter **6**, 873 (1994)
56. D. Valencia, E. Wilson, Z. Jiang, G.A. Valencia-Zapata, K.C. Wang, G. Klimeck, M. Povolotskyi, Grain-boundary resistance in copper interconnects: From an atomistic model to a neural network. Phys. Rev. Appl. **9**, 044005 (2018)
57. X.-G. Zhang, K. Varga, S.T. Pantelides, Generalized Bloch theorem for complex periodic potentials: a powerful application to quantum transport calculations. Phys. Rev. B **76**, 035108 (2007)
58. L. Lu, Y.F. Shen, X.H. Chen, L.H. Qian, K. Lu, Ultrahigh strength and high electrical conductivity in copper. Science **304**, 422 (2004)
59. B.H. Zhou, Y. Xu, S. Wang, G. Zhou, K. Xia, An ab initio investigation on boundary resistance for metallic grains. Solid State Commun. **150**, 1422 (2010)
60. J. Lee, M. Lamarche and V. P. Georgiev, "The First-Priniple Simulation Study on the Specific Grain Boundary Resistivity in Copper Interconnects," *2018 IEEE 13th Nanotechnology Materials and Devices Conference (NMDC)*, Portland, OR, 14–17 Oct. 2018, Paper #8605907, pp. 1–4 (2018); DOI: https://doi.org/10.1109/NMDC.2018.8605907
61. H. Dixit, A. Konar, R. Pandey, J. Cho and F. Benistant, Analyzing the Impact of Grain Boundary Scattering on the Metal Resistivity: First-Principles Study of Symmetric Tilt Grain Boundaries in Copper. In: R. K. Sharma and D. S. Rawal (eds.), *The Physics of Semiconductor Devices, Springer Proceedings in Physics* Vol. 215, p. 691 (2019); https://doi.org/10.1007/978-3-319-97604-4_107
62. C. Kittel, *Introduction to Solid State Physics*, 6th edn. (Wiley, New York, 1986)
63. B. Feldman, S. Park, M. Haverty, S. Shankar, S.T. Dunham, Simulation of grain boundary effects on electronic transport in metals, and detailed causes of scattering. Phys. Status Solidi **247**, 1791 (2010)
64. J.M. Rickman, K. Barmak, Simulation of electrical conduction in thin polycrystalline metallic films: Impact of microstructure. J. Appl. Phys. **114**, 133703 (2013)
65. R. Landauer, Spatial variation of currents and fields due to localized scatterers in metallic conduction. IBM J. Res. Dev. **1**, 223 (1957)
66. C.S. Smith, L. Guttman, Measurement of internal boundaries in three-dimensional structures by random sectioning. J. Metals **5**, 81 (1953)
67. J.H. Hensler, The relation between grain section and grain size. J. Inst. Metals **96**, 190 (1968)
68. R.T. DeHoff, F. Rhines, *Quantitative Microscopy* (McGraw-Hill, New York, 1968)
69. J.L. McCrea, K.T. Aust, G. Palumbo, U. Erb, Electrical resistivity as a characterization tool for nanocrystalline metals. MRS Symp. Proc. **581**, 461 (2000)
70. J.L. McCrea, The effect of temperature on the electrical resistivity of ellectrodeposited nanocrystalline materials (Ph.D. Thesis, University of Toronto, Canada, 2001); unpublished, available at https://www.collectionscanada.gc.ca/obj/s4/f2/dsk3/ftp04/NQ59029.pdf
71. A.F. Mayadas, Intrinsic resistivity and electron mean free path in aluminum films. J. Appl. Phys. **39**, 4241 (1968)

72. A.F. Mayadas, M. Shatzkes, J.F. Janak, Electrical resistivity model for polycrystalline films: the case of specular reflection at external surfaces. Appl. Phys. Lett. **14**, 345 (1969)
73. B.D. Cullity and S.R. Stock, *Elements of X-ray Diffraction* (Third Edition, Prentice Hall, Upper Saddle River, New Jersey, U.S:A., 2001)
74. R. Mitra, T. Ungár, J.R. Weertman, A comparison of grain size measurements by X-ray diffraction and transmission electron microscopy methods. Trans. Indian Inst. Met. **58**, 1125 (2005)
75. J. Gubicza, *X-Ray Line Profile Analysis in Materials Science* (IGI-Global, Hershey, PA, 2014)
76. T. Kolonits, P. Jenei, B.G. Tóth, Z. Czigány, J. Gubicza, L. Péter, I. Bakonyi, Characterization of defect structure in electrodeposited nanocrystalline Ni films. J. Electrochem. Soc. **163**, D107 (2016)
77. T. Kolonits, P. Jenei, L. Péter, I. Bakonyi, Z. Czigány, J. Gubicza, Effect of bath additives on the microstructure, lattice defect density and hardness of electrodeposited nanocrystalline Ni films. Surf. Coat. Technol. **349**, 611 (2018)
78. T. Kino, T. Endo, S. Kawata, Deviations from Matthiessen's rule of the electrical resistivity of dislocations in aluminum. J. Phys. Soc. Japan **36**, 698 (1974)
79. L.H. Qian, Q.H. Lu, W.J. Kong, K. Lu, Electrical resistivity of fully-relaxed grain boundaries in nanocrystalline Cu. Scripta Mater. **50**, 1407 (2004)
80. X.H. Chen, L. Lu, K. Lu, Electrical resistivity of ultrafine-grained copper with nanoscale growth twins. J. Appl. Phys. **102**, 083708 (2007)
81. P.V.P. Madduri, S.N. Kaul, Magnon-induced interband spin-flip scattering contribution to resistivity and magnetoresistance in a nanocrystalline itinerant-electron ferromagnet: Effect of crystallite size. Phys. Rev. B **95**, 184402 (2017)
82. N.C. Halder, C.N.J. Wagner, Separation of particle size and lattice strain in integral breadth measurements. Acta Cryst. **20**, 312 (1966)
83. P. Wissmann, On the influence of the polycrystalline structure on the electrical resistivity of evaporated nickel films. Thin Solid Films **5**, 329 (1970) (**In German**)
84. C. Reale, Electrical properties of vacuum deposited nickel films. Phys. Lett A **24**, 145 (1967)
85. C. Nacereddine, A. Layadi, A. Guittoum, S.M. Chérif, T. Chauveau, D. Billet, J. Ben Youssef, A. Bourzami, M.H. Bourahli, Structural, electrical and magnetic properties of evaporated Ni/Cu and Ni/glass thin films. Mater. Sci. Eng. B **136**, 197 (2007)
86. M. Hemmous, A. Layadi, A. Guittoum, A. Bourzami, A. Benabbas, Effect of deposition rate and thickness on the structural and electrical properties of evaporated Ni/glass and Ni/Si (1 0 0) thin films. Microelectr. J. **39**, 1545 (2008)
87. K.M. Mannan, K.R. Karim, Grain boundary contribution to the electrical conductivity of polycrystalline Cu films. J. Phys. F **5**, 1687 (1975)
88. G. Palumbo, S.J. Thorpe, K.T. Aust, On the contribution of triple junctions to the structure and properties of nanocrystalline materials. Scripta Met. Mater. **24**, 1347 (1990)
89. M. Shimoji, *Liquid Metals* (Academic Press, London, 1977), p. 267